FEDERAL RESERVE BANK OF SAN FRANCISCO

WORKING PAPER SERIES

# A Post-Pandemic New Normal for Interest Rates in Emerging Bond Markets? Evidence from Chile

Luis Ceballos
University of San Diego

Jens H. E. Christensen
Federal Reserve Bank of San Francisco

Damian Romero
Banco Central de Chile

February 2024

Working Paper 2024-04

https://doi.org/10.24148/wp2024-04

**Suggested citation:**

Ceballos, Luis, Jens H. E. Christensen, and Damian Romero. 2024. "A Post-Pandemic New Normal for Interest Rates in Emerging Bond Markets? Evidence from Chile." Federal Reserve Bank of San Francisco Working Paper 2024-04. https://doi.org/10.24148/wp2024-04

# A Post-Pandemic New Normal for Interest Rates in Emerging Bond Markets? Evidence from Chile

Luis Ceballos

Jens H. E. Christensen

Damian Romero

**Abstract**

Before the COVID-19 pandemic, researchers intensely debated the extent of the decline in the so-called equilibrium or natural rate of interest. Given the recent sharp increase in interest rates, we revisit this question in an emerging bond market context and offer a Chilean perspective using a dynamic term structure finance model estimated directly on the prices of individual Chilean inflation-indexed bonds with adjustments for bond-specific liquidity risk and real term premia. We estimate that the equilibrium real rate in Chile fell about 2 and a half percentage points in the 2003-2022 period and has remained low since then.

*JEL Classification:* C32, E43, E52, G12

*Keywords:* affine arbitrage-free term structure model, financial market frictions, monetary policy, rstar

Luis Ceballos (luisceballos@sandiego.edu), Jens H. E. Christensen (jens.christensen@sf.frb.org), Damian Romero (dromeroc@bcentral.cl). Corresponding author: Jens Christensen, Economic Research Department, Federal Reserve Bank of San Francisco, 101 Market Street (MS 1130), San Francisco, CA 94105. We thank participants at el Primer Congreso Internacional de Investigación de Ingeniería Económica, Ingeniería Estadística y Ciencias Sociales for helpful comments. Furthermore, we thank seminar participants at the Universidad Técnica Federico Santa María and the Central Bank of Chile for helpful comments. The views in this paper are solely the responsibility of the authors and do not necessarily reflect those of others in the Federal Reserve System or at the Central Bank of Chile.

This version: February 21, 2024.

# 1 Introduction

Before the COVID-19 pandemic, the general level of interest rates in many developed countries had gradually declined over the previous several decades. In the 1980s and 1990s, falling inflation expectations played a key role in this decline. But in the 2000s and 2010s, actual inflation as well as survey-based measures of longer-run inflation expectations were relatively stable in many countries, including in many emerging market economies. Therefore, researchers argued that the decline in interest rates in the later decades reflected a variety of longer-run real-side factors instead of nominal ones. These real factors—such as slower productivity growth and an aging population—affect global saving and investment and can push down nominal and real yield curves by lowering the steady-state level of the safe short-term real interest rate.[1] This steady-state real rate is often called the equilibrium or natural or neutral rate of interest and is commonly defined as the short-term real rate of return that would prevail in the absence of transitory disturbances. However, some dismissed the evidence for a new lower equilibrium real rate. They downplayed the role of persistent real-side factors and argued that yields had been held down by temporary factors such as the headwinds from credit deleveraging in the aftermath of the Global Financial Crisis of 2008-2009.[2] However, the surge in inflation and interest rates that followed the post-pandemic economic reopening, which was severely exacerbated by Russia's war on Ukraine launched in February 2022, has underscored the need to better understand how steady state real rates have responded to these extraordinary economic shocks. While most of the existing debate has focused on estimates drawn from *macroeconomic* models and data, we instead follow Christensen and Rudebusch (2019, henceforth CR) and use *financial* models. Moreover, we rely on inflation-indexed bond prices from Chile for our analysis and therefore provide an emerging market perspective on any post-pandemic new normal for interest rates.

The issue of whether there have been persistent shifts in the equilibrium real rate is of general importance. For investors, the steady-state level of the real short rate serves as an anchor for projections of the future discount rates used in valuing assets (e.g., Clarida 2014). For policymakers and researchers, the equilibrium or natural rate of interest is a policy lodestar that provides a neutral benchmark to calibrate the stance of monetary policy: Monetary policy is expansionary if the short-term real interest rate lies below the natural rate and contractionary if it lies above. A good estimate of the equilibrium real rate is also necessary to operationalize popular monetary policy rules such as the Taylor rule.[3] More

[1]For example, see Rachel and Smith (2015), Gagnon et al. (2016), Hamilton et al. (2016), Laubach and Williams (2016), and Pescatori and Turunen (2016), among many others.

[2]For example, see Kiley (2015), Lo and Rogoff (2015), and Taylor and Wieland (2016).

[3]For a recent discussion of the connection between the natural rate of interest and monetary policy in Chile, see, e.g., Box II.2 in the December 2022 Monetary Policy Report of the Central Bank of Chile. For research on the role of the natural rate in monetary policy, see Rudebusch (2001), Orphanides and Williams (2002),

recently, the post-pandemic spike in interest rates globally has given rise to intense policy debates about whether interest rates will hold steady at the new higher levels or revert back towards their pre-pandemic lows.[4]

Against this backdrop of unsettled questions surrounding the persistent decline in interest rates in the decades before the pandemic and the recent signs of a potential reversal, Chilean yield data is unique in that the Chilean government was one of the first to issue inflation-indexed bonds as early as the mid-1960s. However, because limited data is available for the early years of trading, we start our sample in 2003 similar to De Pooter et al. (2014). These securities have coupon and principal payments indexed to the Chilean Consumer Price Index (CPI) and provide compensation to investors for the erosion of purchasing power due to price inflation.[5] Therefore, their bond prices can be expressed directly in terms of real yields. We assume that the longer-term expectations embedded in the bond prices reflect financial market participants' views about the steady state of the economy, including the natural rate of interest. This long sample allows us to provide a full 20-year perspective on the components that have pushed Chilean real yields lower in previous decades and given rise to any possible recent reversal. Besides its length, a Chilean study offers additional advantages. First, Chile has fairly liquid markets for inflation-indexed government debt. Second, with maturities of up to 30 years, the inflation-indexed bond market contains significant forward-looking information and hence is likely to provide clear evidence for the questions at hand. Third, by relying on inflation-indexed bonds, we avoid any issues related to the zero lower bound that applies to the Chilean overnight rate and other nominal interest rates. Furthermore, as the underlying factors affecting long-term interest rates are likely global in nature—such as worldwide demographic shifts, changes in productivity trends, or persistent adjustments to global supply chains in the post-pandemic world—the Chilean government bond market may well be as informative as any other emerging sovereign bond market. Thus, we think of the data as being representative for emerging bond markets more broadly. Finally, the Chilean government holds an A+ credit rating or higher with a stable outlook from all major rating agencies. Hence, there is a minimum of credit risk to account for in our Chilean bond price data.

Despite all these advantages, using inflation-indexed bonds for measuring the steady-state short-term real interest rate has its own empirical challenges. One problem is that inflation-indexed bond prices include a real term premium. Given the generally upward slope of the Chilean inflation-indexed bond yield curve, the real term premium is presumably usually positive. However, little is known with certainty about its size or variability. In addition, despite the fairly large notional amount of outstanding inflation-indexed bonds,

Eggertsson et al. (2016), and Hamilton et al. (2016), among many others.

[4]See, for example, Blanchard (2023) and Summers (2023).

[5]The CPI is also the price index targeted by the Central Bank of Chile for monetary policy purposes.

these securities inherently face appreciable liquidity risk for structural reasons as argued by Cardozo and Christensen (2023). Since they provide a hedge against inflation risk, they are likely to be much less traded than nominal bonds. Also, because this hedge argument only applies to domestic investors whose consumption expenditures track the local CPI, foreigners will not benefit from holding these securities. As a consequence, the trading of inflation-indexed bonds ends up being concentrated among patient domestic buy-and-hold investors like pension funds and insurance companies. Presumably, investors require a premium for bearing the liquidity risk associated with holding inflation-indexed bonds, but the extent and time variation of this liquidity premium deserve further examination.[6]

To estimate the natural rate of interest in the presence of liquidity and real term premia, we use an arbitrage-free dynamic term structure model of real yields augmented with a liquidity risk factor. The identification of the liquidity risk factor comes from its unique loading for each individual security as in Andreasen et al. (2021, henceforth ACR). Our analysis uses prices of individual bonds rather than the more usual input of yields from fitted synthetic curves. The underlying mechanism assumes that, over time, an increasing proportion of the outstanding inventory is locked up in buy-and-hold portfolios. Given forward-looking investor behavior, this lockup effect means that a particular bond's sensitivity to the marketwide liquidity factor will vary depending on how seasoned and how close to maturity the bond is. In a careful study of nominal Treasuries, Fontaine and Garcia (2012) also find a pervasive liquidity factor that affects all bond prices, with loadings that vary with the maturity and age of each bond. By observing a cross section of bond prices over time—each with a different time since issuance and time to maturity—we can identify the overall liquidity factor and each bond's loading on that factor. This technique is particularly useful for analyzing inflation-indexed debt when only a limited sample of bonds may be available, as in the early years of our sample.[7]

The theoretical arbitrage-free formulation of the model also provides identification of a time-varying real term premium in the pricing of inflation-indexed bonds. Identifying the liquidity premium and real term premium allows us to estimate the underlying frictionless real rate term structure and the natural rate of interest, which we measure as the average expected real short rate over a five-year period starting five years ahead, as in CR. Our preferred estimate of the natural rate of interest, $r_t^*$, is shown in Figure 1 along with ten-year nominal and real Chilean government bond yields. Both nominal and real long-term yields trended down together until 2020 followed by a joint sharp reversal, and this concurrence suggests little net change in inflation expectations or the inflation risk premium. In contrast,

[6]A large literature has emphasized liquidity risk as an important component in the pricing of U.S. Treasury inflation-protected securities (TIPS). See, for example, Sack and Elsasser (2004), Campbell et al. (2009), Dudley et al. (2009), Gürkaynak et al. (2010), Fleckenstein et al. (2014), Driessen, et al. (2016), and Pflueger and Viceira (2016).

[7]Finlay and Wende (2012) examine prices from a limited number of Australian inflation-indexed bonds but do not account for liquidity premia.

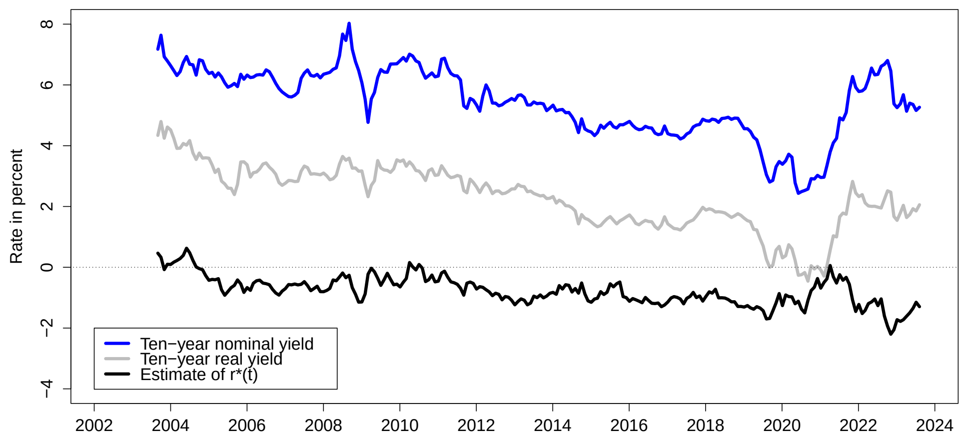


Figure 1: **Long-Term Nominal and Real Yields and an Estimate of r**$^*$
Ten-year nominal and real yields and our preferred AFNS-L model estimate of the equilibrium real short rate, $r_t^*$, i.e., the 5- to 10-year risk-neutral real rate.

the estimated equilibrium real rate fell from just below 0.5 percent to below -2 percent during the 2003-2022 period and has remained low since then. Accordingly, our results show that the reduction in the natural rate of interest can account for about half of the 4-percentage-point decline in longer-term Chilean yields during the 2003-2020 period. Crucially, our results suggest that the recent increases in real interest rates in Chile are driven by spikes in the liquidity and term premia of inflation-indexed bond prices, leaving the natural rate little affected despite the yield increases. Furthermore, model projections suggest only a gradual reversal in coming years.

Our analysis also documents the existence of large and time-varying liquidity risk premia in the Chilean inflation-indexed bond prices. Regression analysis with a large number of control variables shows that the average liquidity premium series is significantly negatively correlated with the size of the indexed bond market measured as a share of nominal GDP, while it is significantly positively correlated with the share of the market held by buy-and-hold investors as proxied through the holdings of pension funds. Hence, market size and concentration are two key determinants of investors' perceptions about the liquidity risk in this market. We take these results to imply that there are material frictions to the trading of these securities consistent with the general arguments provided in Cardozo and Christensen (2023). Moreover, they underscore the importance of the liquidity adjustment for our results.

The analysis in this paper relates to several important strands of literature. Most directly, it speaks to the burgeoning literature on measurement of the natural rate of interest. Second, our estimates of the real yield curve that would prevail without trading frictions have implications for asset pricing analysis on the true slope of the real yield curve. Furthermore, our results relate to research on financial market liquidity premia. Finally, the paper contributes to the rapidly growing literature about the economic consequences of the COVID-19 pandemic.

The remainder of the paper is organized as follows. Section 2 contains a description of the Chilean inflation-indexed bond data, while Section 3 details the no-arbitrage term structure models we use and presents the empirical results. Section 4 validates the estimated real bond-specific liquidity premia and examines their determinants, while Section 5 analyzes our bond-based estimate of the natural rate and compares it with other measures. Finally, Section 6 concludes.

## 2 The Chilean Inflation-Indexed Bond Data

The Chilean government issued its first inflation-indexed bonds back in the 1960s (see Shiller 2003). These bonds are known as bonos tesoreria UF, or BTUs for short, and their cash flow is measured in a unit known as the "Unidad de Fomento." At the end of our sample on July 31, 2023, the net outstanding uplifted amount of BTUs was 32,660 billion Chilean pesos, which accounted for 48.8 percent of all marketable Chilean government securities, and their average maturity was 9.58 years.[8] The total number of outstanding inflation-indexed bonds over time in our sample is shown as a solid gray line in Figure 2(a). At the end of our sample period—which runs from August 2003 to July 2023—24 bonds were outstanding. However, as noted by Gürkaynak et al. (2010) and ACR, prices of inflation-indexed bonds near their maturity tend to be somewhat erratic because of the indexation lag in their payoffs. Therefore, to facilitate model estimation, we drop inflation-indexed bonds from our sample when they have less than one year to maturity. Using this cutoff, the number of bonds in the sample is modestly reduced, as shown with a solid black line in Figure 2(a). Finally, Tables 1 and 2 contain the contractual details of all 72 BTUs in our data as well as the number of monthly observations for each.

Since the early 2000s the Chilean government has issued a variety of inflation-indexed bonds with original maturities ranging from 2 years to 31 years. The maturity distribution of the 72 bonds in our sample is shown in Figure 2(b). Each bond is represented by a single downward-sloping line that plots its remaining years to maturity for each date. For the five- to ten-year maturities of particular interest for our analysis, the universe of bonds provides good coverage throughout our sample.

Figure 3 shows the yield-to-maturity series for all inflation-indexed bonds in our sample at the end of each month from August 2003 to July 2023. Note the following regarding these

[8] The data is from Bloomberg and Riskamerica (www.riskamerica.com).

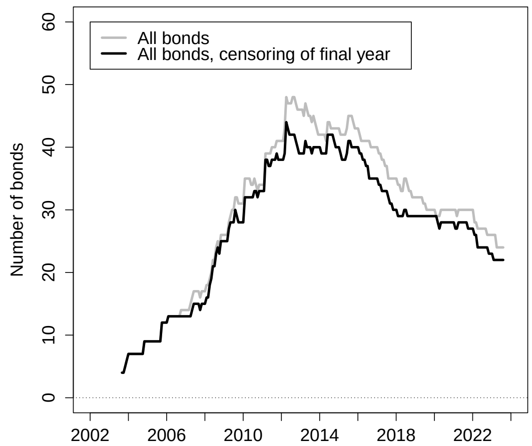


(a) Number of inflation-indexed bonds

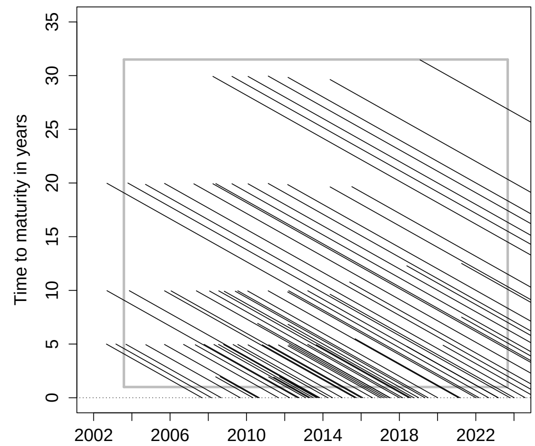


(b) Distribution of inflation-indexed bonds

Figure 2: **Overview of the Chilean Inflation-Indexed Bond Data**
Panel (a) reports the number of outstanding inflation-indexed bonds at a given point in time. Panel (b) shows the maturity distribution of all inflation-indexed bonds issued since 2002. The solid gray rectangle indicates the sample used in our analysis, where the sample is restricted to start on August 31, 2003, and limited to inflation-indexed bond prices with more than one year to maturity after issuance.

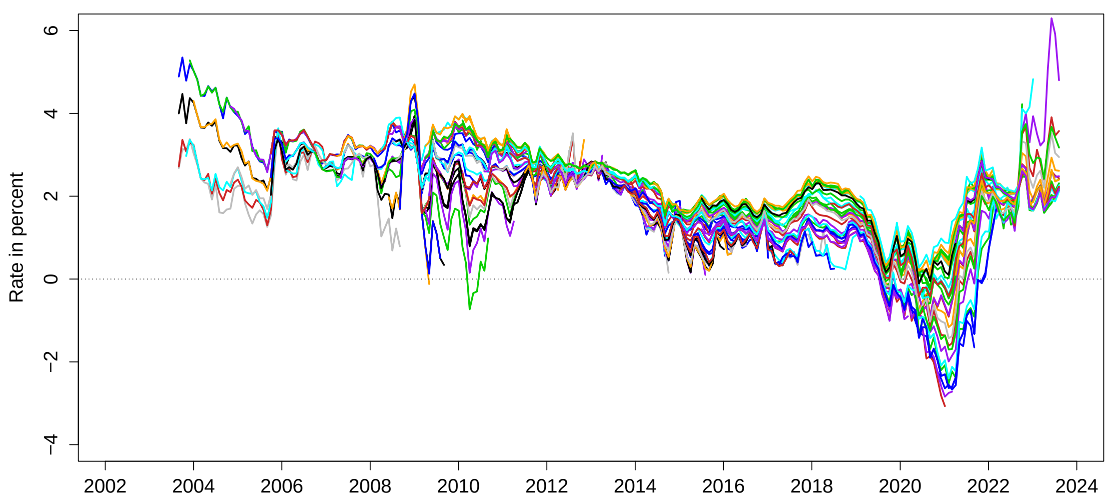


Figure 3: **Yield to Maturity of Chilean Inflation-Indexed Bonds**

yield series. First, the significant persistent decline in real yields over the first 18 years of the sample is clearly visible, as is the rapid retracing of those declines during the last two years

| Inflation-indexed bond | No. obs. | Issuance Date | Issuance amount | Total uplifted amount |
|---|---|---|---|---|
| (1) 5% 9/1/2007 | 37 | 9/1/2002 | 28.5 | 264.3 |
| (2) 5% 9/1/2012 | 97 | 9/11/2002 | 11.3 | 279.7 |
| (3) 5% 9/1/2022 | 217 | 9/11/2002 | 13.5 | 282.7 |
| (4) 5% 3/1/2008 | 43 | 3/1/2003 | 33.6 | 266.8 |
| (5) 5% 9/1/2008 | 47 | 9/9/2003 | 31.8 | 275.6 |
| (6) 4.5% 10/15/2023 | 227 | 10/16/2003 | 119.4 | 718.4 |
| (7) 5% 11/1/2013 | 107 | 11/12/2003 | 8.1 | 255.1 |
| (8) 4.5% 8/1/2024 | 226 | 9/16/2004 | 651.1 | 651.1 |
| (9) 5% 9/1/2009 | 47 | 9/22/2004 | 245.7 | 251.0 |
| (10) 5% 9/1/2010 | 48 | 9/14/2005 | 5.3 | 250.5 |
| (11) 2.1% 9/1/2015 | 108 | 9/15/2005 | 7.6 | 277.2 |
| (12) 2.6% 9/1/2025 | 215 | 9/15/2005 | 24.6 | 397.9 |
| (13) 5% 1/1/2016 | 108 | 1/18/2006 | 10.3 | 265.8 |
| (14) 5% 9/1/2011 | 48 | 9/13/2006 | 22.0 | 219.8 |
| (15) 3% 3/1/2027 | 197 | 3/29/2007 | 36.2 | 366.1 |
| (16) 3% 4/1/2012 | 48 | 4/25/2007 | 45.1 | 270.4 |
| (17) 3% 5/1/2017 | 108 | 5/16/2007 | 37.2 | 204.6 |
| (18) 3% 10/1/2012 | 48 | 10/10/2007 | 45.2 | 284.7 |
| (19) 3% 1/1/2018 | 108 | 1/23/2008 | 37.5 | 505.7 |
| (20) 3% 3/1/2028 | 185 | 3/27/2008 | 36.9 | 745.1 |
| (21) 3% 3/1/2038 | 185 | 3/27/2008 | 36.9 | 618.5 |
| (22) 3% 4/1/2013 | 48 | 4/16/2008 | 50.3 | 379.9 |
| (23) 3% 5/1/2010 | 12 | 5/19/2008 | 23.1 | 269.2 |
| (24) 3% 5/1/2028 | 183 | 5/21/2008 | 43.4 | 415.3 |
| (25) 3% 7/1/2013 | 48 | 7/12/2008 | 38.8 | 604.2 |
| (26) 3% 7/1/2018 | 108 | 7/16/2008 | 68.4 | 612.2 |
| (27) 3% 8/1/2010 | 12 | 8/12/2008 | 31.8 | 410.1 |
| (28) 3% 10/1/2013 | 48 | 10/17/2008 | 48.5 | 219.4 |
| (29) 3% 10/1/2018 | 108 | 10/30/2008 | 58.0 | 265.9 |
| (30) 3% 3/1/2029 | 173 | 3/26/2009 | 36.2 | 359.9 |
| (31) 3% 3/1/2039 | 173 | 3/26/2009 | 36.2 | 361.7 |
| (32) 3% 4/1/2014 | 48 | 4/17/2009 | 23.6 | 47.2 |
| (33) 3% 5/1/2019 | 108 | 5/28/2009 | 26.6 | 26.6 |
| (34) 3% 7/1/2014 | 48 | 7/15/2009 | 64.9 | 324.4 |
| (35) 3% 7/1/2019 | 108 | 7/15/2009 | 174.4 | 697.7 |
| (36) 3% 1/1/2015 | 48 | 1/28/2010 | 61.6 | 837.3 |

Table 1: **Sample of Chilean Inflation-Indexed Bonds**
The table reports the characteristics, first issuance date and amount, and total amount issued in billions of Chilean pesos either at maturity or as of July 31, 2023, for the sample of Chilean inflation-indexed bonds. Also reported are the number of monthly observation dates for each bond during the sample period from August 31, 2003, to July 31, 2023.

of the sample. Chilean long-term real yields were above 4 percent in the early 2000s and had dropped to near zero by late 2020. Second, business cycle variation in the shape of the yield

| Inflation-indexed bond | No. obs. | Issuance Date | Issuance amount | Total uplifted amount |
|---|---|---|---|---|
| (37) 3% 1/1/2020 | 108 | 1/21/2010 | 70.8 | 1,824.1 |
| (38) 3% 1/1/2030 | 163 | 1/28/2010 | 72.3 | 1,700.1 |
| (39) 3% 1/1/2040 | 163 | 1/28/2010 | 72.3 | 1,700.1 |
| (40) 3% 7/1/2017 | 72 | 7/29/2010 | 106.7 | 1,120.0 |
| (41) 3% 10/1/2015 | 48 | 10/26/2010 | 25.4 | 202.8 |
| (42) 3% 2/1/2013 | 12 | 2/25/2011 | 45.6 | 150.5 |
| (43) 3% 2/1/2016 | 48 | 2/25/2011 | 76.9 | 845.8 |
| (44) 3% 2/1/2021 | 108 | 2/16/2011 | 58.3 | 1,281.6 |
| (45) 3% 2/1/2031 | 150 | 2/17/2011 | 108.5 | 1,012.9 |
| (46) 3% 2/1/2041 | 150 | 2/17/2011 | 108.5 | 1,012.8 |
| (47) 3% 5/1/2013 | 11 | 6/1/2011 | 55.1 | 183.5 |
| (48) 3% 8/1/2016 | 47 | 9/1/2011 | 65.4 | 575.2 |
| (49) 3% 9/1/2013 | 12 | 9/21/2011 | 46.1 | 170.5 |
| (50) 3% 1/1/2017 | 46 | 3/1/2012 | 55.3 | 266.5 |
| (51) 3% 1/1/2019 | 70 | 3/1/2012 | 33.1 | 132.3 |
| (52) 3% 1/1/2022 | 107 | 2/23/2012 | 74.4 | 838.8 |
| (53) 3% 1/1/2032 | 138 | 2/23/2012 | 54.3 | 922.8 |
| (54) 3% 1/1/2042 | 137 | 3/1/2012 | 54.3 | 939.6 |
| (55) 3% 3/1/2017 | 48 | 3/21/2012 | 42.2 | 332.6 |
| (56) 3% 3/1/2022 | 108 | 3/14/2012 | 47.3 | 725.8 |
| (57) 3% 7/1/2017 | 48 | 7/11/2012 | 41.3 | 330.7 |
| (58) 3% 3/1/2018 | 48 | 3/12/2013 | 616.7 | 616.7 |
| (59) 3% 3/1/2023 | 108 | 3/13/2013 | 390.7 | 390.8 |
| (60) 3% 8/1/2018 | 48 | 8/21/2013 | 73.4 | 220.3 |
| (61) 3% 1/1/2024 | 104 | 5/14/2014 | 90.4 | 976.6 |
| (62) 3% 1/1/2034 | 111 | 5/14/2014 | 86.8 | 813.9 |
| (63) 3% 1/1/2044 | 111 | 5/14/2014 | 32.6 | 6,541.7 |
| (64) 1.5% 3/1/2021 | 57 | 9/3/2015 | 747.0 | 3,765.0 |
| (65) 1.5% 3/1/2026 | 99 | 5/22/2015 | 1121.3 | 6,594.6 |
| (66) 2% 3/1/2035 | 79 | 7/3/2015 | 922.4 | 5,453.3 |
| (67) 1.3% 3/1/2023 | 46 | 5/18/2018 | 802.7 | 2,163.2 |
| (68) 1.9% 9/1/2030 | 63 | 5/18/2018 | 716.9 | 4,000.6 |
| (69) 2.1% 7/15/2050 | 55 | 1/26/2019 | 227.9 | 2,902.2 |
| (70) 0% 3/1/2025 | 40 | 4/10/2020 | 176.5 | 1,771.0 |
| (71) 0% 10/1/2028 | 29 | 3/29/2021 | 151.9 | 1,848.0 |
| (72) 0% 10/1/2033 | 29 | 3/29/2021 | 151.9 | 2,916.6 |

Table 2: **Sample of Chilean Inflation-Indexed Bonds Cont.**
The table reports the characteristics, first issuance date and amount, and total amount issued in billions of Chilean pesos either at maturity or as of July 31, 2023, for the sample of Chilean inflation-indexed bonds. Also reported are the number of monthly observation dates for each bond during the sample period from August 31, 2003, to July 31, 2023.

curve is pronounced around these trends. The yield curve tends to flatten ahead of recessions and steepen during the initial phase of economic recoveries. These characteristics are the

| Maturity in months | First P.C. | Second P.C. | Third P.C. |
|---|---|---|---|
| 24 | 0.46 | 0.64 | -0.58 |
| 36 | 0.41 | 0.34 | 0.44 |
| 60 | 0.37 | 0.03 | 0.50 |
| 84 | 0.36 | -0.14 | 0.26 |
| 120 | 0.35 | -0.28 | -0.01 |
| 180 | 0.35 | -0.40 | -0.23 |
| 240 | 0.34 | -0.46 | -0.32 |
| % explained | 88.20 | 9.91 | 1.73 |

Table 3: **Factor Loadings of Chilean Inflation-Indexed Bond Yields**
The top rows show the eigenvectors corresponding to the first three principal components (PC). Put differently, they show how bond yields at various maturities load on the first three principal components. In the final row the proportion of all bond yield variability explained by each principal component is shown. The data are daily Chilean zero-coupon inflation-indexed bond yields from August 1, 2003, to July 31, 2023, a total of 5,075 observations for each yield series.

practical motivation behind our choice of using a three-factor model for the frictionless part of the Chilean yield curve, adopting an approach similar to what is standard for U.S. and U.K. nominal yield data; see Christensen and Rudebusch (2012).

To support that choice more formally, we note that researchers have typically found that three factors are sufficient to model the time variation in the cross section of U.S. Treasury yields (e.g., Litterman and Scheinkman 1991). To perform a similar analysis based on our sample of Chilean inflation-indexed bond prices, we construct synthetic zero-coupon bond yields by fitting the flexible Svensson (1995) yield curve to the set of inflation-indexed bond prices observed for each observation date.[9] To have a yield panel representative of the underlying bonds in our sample, we include yields for seven constant maturities: 2, 3, 5, 7, 10, 15, and 20 years. The data series are daily, covering the period from August 1, 2003, to July 31, 2023.

The result of a principal components analysis of the yield panel is reported in Table 3. The top panel reports the eigenvectors that correspond to the first three principal components. The first principal component accounts for 88.2 percent of the variation in the bond yields, and its loading across maturities is uniformly positive. Thus, similar to a level factor, a shock to this component changes all yields in the same direction irrespective of maturity. The second principal component accounts for 9.9 percent of the variation in these data and has sizable positive loadings for the shorter maturities and sizable negative loadings for the long maturities. Thus, similar to a slope factor, a shock to this component steepens or flattens the yield curve. Finally, the third component, which accounts for 1.7 percent of the variation,

[9]Technically, we proceed as described in Andreasen et al. (2019).

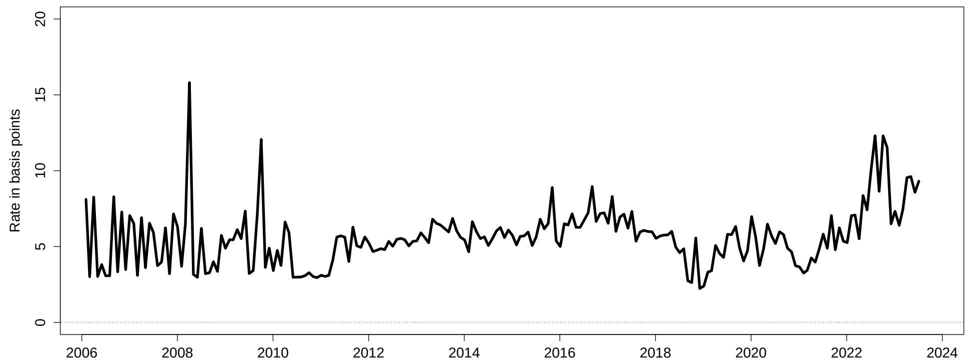


Figure 4: **Bid-Ask Spreads of Chilean Inflation-Indexed Bonds**

has a hump-shaped factor loading as a function of maturity, which is naturally interpreted as a curvature factor. These three factors combined account for 99.84 percent of the total variation. This motivates our choice to focus on the Nelson and Siegel (1987) model with its level, slope, and curvature factors for modeling this sample of Chilean inflation-indexed bond prices. However, for theoretical consistency, we use the arbitrage-free version of this class of models derived in Christensen et al. (2011). Furthermore, to explain the remaining variation in the bond yield data not accounted for by the level, slope, and curvature factors, we augment the model with a risk factor to allow for bond-specific liquidity risk premia using the approach described in ACR and detailed in Section 3. Importantly, we stress that the estimated state variables in our model are *not* identical to the principal component factors discussed here, but estimated through Kalman filtering.[10]

## 2.1 Bid-Ask Spreads of Chilean Inflation-Indexed Government Bonds

To shed light on the trading frictions in the market for Chilean inflation-indexed bonds, we compute the average bid-ask spread of the bonds in our sample for the available period, which starts in 2006. The resulting series is shown in Figure 4. There are two key takeaways. First, with an average level of bid-ask spreads of around 5.6 basis points, the trading of these securities is indeed associated with some amount of liquidity risk. Second, the occasional large spikes in the bid-ask spreads of inflation-indexed bonds is a sign that the liquidity risk of these securities can be elevated at times, and we want to account for that in our analysis.

The empirical question we are interested in is to what extent the decline in the inflation-indexed bond yields through the end of 2020 and the subsequent sharp reversal represent

[10]A number of recent papers use principal components as state variables. Joslin et al. (2011) is an early example.

variation in the natural real rate or are driven by other factors such as term or other bond-specific liquidity risk premia.

# 3 Model Estimation and Results

In this section, we first describe how we model yields in a world without any frictions to trading. This model of frictionless dynamics is fundamental to our analysis. We then detail the augmented model that accounts for the liquidity premia in the inflation-indexed bond yields. This is followed by a description of the restrictions imposed to achieve econometric identification of this model and its estimation. We end the section with a brief summary of our estimation results.

## 3.1 A Frictionless Arbitrage-Free Model of Real Yields

To capture the fundamental or frictionless factors operating the Chilean real yield curve, we choose to focus on the tractable affine dynamic term structure model introduced in Christensen et al. (2011).[11]

In this arbitrage-free Nelson-Siegel (AFNS) model, the state vector is denoted by $X_t = (L_t, S_t, C_t)$, where $L_t$ is a level factor, $S_t$ is a slope factor, and $C_t$ is a curvature factor. The instantaneous risk-free real rate is defined as

$$r_t = L_t + S_t. \tag{1}$$

The risk-neutral (or $\mathbb{Q}$-) dynamics of the state variables are given by the stochastic differential equations[12]

$$\begin{pmatrix} dL_t \\ dS_t \\ dC_t \end{pmatrix} = \begin{pmatrix} 0 & 0 & 0 \\ 0 & -\lambda & \lambda \\ 0 & 0 & -\lambda \end{pmatrix} \begin{pmatrix} L_t \\ S_t \\ C_t \end{pmatrix} dt + \Sigma \begin{pmatrix} dW_t^{L,\mathbb{Q}} \\ dW_t^{S,\mathbb{Q}} \\ dW_t^{C,\mathbb{Q}} \end{pmatrix}, \tag{2}$$

where $\Sigma$ is the constant covariance (or volatility) matrix. Based on this specification of the $\mathbb{Q}$-dynamics, zero-coupon real bond yields preserve the Nelson-Siegel factor loading structure as

$$y_t(\tau) = L_t + \left(\frac{1-e^{-\lambda\tau}}{\lambda\tau}\right) S_t + \left(\frac{1-e^{-\lambda\tau}}{\lambda\tau} - e^{-\lambda\tau}\right) C_t - \frac{A(\tau)}{\tau}, \tag{3}$$

where $\frac{A(\tau)}{\tau}$ is a convexity term that adjusts the functional form in Nelson and Siegel (1987)

[11] Although the model is not formulated using the canonical form of affine term structure models introduced by Dai and Singleton (2000), it can be viewed as a restricted version of the canonical Gaussian model; see Christensen et al. (2011) for details.

[12] As discussed in Christensen et al. (2011), with a unit root in the level factor, the model is not arbitrage-free with an unbounded horizon; therefore, as is often done in theoretical discussions, we impose an arbitrary maximum horizon.

to ensure absence of arbitrage (see Christensen et al. 2011).

To complete the description of the model and to implement it empirically, we will need to specify the risk premia that connect these factor dynamics under the $\mathbb{Q}$-measure to the dynamics under the real-world (or physical) $\mathbb{P}$-measure. It is important to note that there are no restrictions on the dynamic drift components under the empirical $\mathbb{P}$-measure beyond the requirement of constant volatility. To facilitate empirical implementation, we use the essentially affine risk premium specification introduced in Duffee (2002). In the Gaussian framework, this specification implies that the risk premia $\Gamma_t$ depend on the state variables; that is,

$$\Gamma_t = \gamma^0 + \gamma^1 X_t,$$

where $\gamma^0 \in \mathbf{R}^3$ and $\gamma^1 \in \mathbf{R}^{3\times 3}$ contain unrestricted parameters.

Thus, the resulting unrestricted three-factor AFNS model has $\mathbb{P}$-dynamics given by

$$\begin{pmatrix} dL_t \\ dS_t \\ dC_t \end{pmatrix} = \begin{pmatrix} \kappa_{11}^{\mathbb{P}} & \kappa_{12}^{\mathbb{P}} & \kappa_{13}^{\mathbb{P}} \\ \kappa_{21}^{\mathbb{P}} & \kappa_{22}^{\mathbb{P}} & \kappa_{23}^{\mathbb{P}} \\ \kappa_{31}^{\mathbb{P}} & \kappa_{32}^{\mathbb{P}} & \kappa_{33}^{\mathbb{P}} \end{pmatrix} \left( \begin{pmatrix} \theta_1^{\mathbb{P}} \\ \theta_2^{\mathbb{P}} \\ \theta_3^{\mathbb{P}} \end{pmatrix} - \begin{pmatrix} L_t \\ S_t \\ C_t \end{pmatrix} \right) dt + \Sigma \begin{pmatrix} dW_t^{L,\mathbb{P}} \\ dW_t^{S,\mathbb{P}} \\ dW_t^{C,\mathbb{P}} \end{pmatrix}.$$

This is the transition equation in the Kalman filter estimation.

### 3.2 An Arbitrage-Free Model of Real Yields with Liquidity Risk

In this section, we augment the frictionless model introduced above to account for the liquidity premium of the inflation-indexed bond prices we use in the empirical analysis. To do so, let $X_t = (L_t, S_t, C_t, X_t^{liq})$ denote the state vector of the four-factor model with liquidity risk premium adjustment and refer to it as the AFNS-L model. As in the non-augmented model, we let the frictionless instantaneous real risk-free rate be defined by equation (1), while the risk-neutral dynamics of the state variables used for pricing are given by

$$\begin{pmatrix} dL_t \\ dS_t \\ dC_t \\ dX_t^{liq} \end{pmatrix} = \begin{pmatrix} 0 & 0 & 0 & 0 \\ 0 & \lambda & -\lambda & 0 \\ 0 & 0 & \lambda & 0 \\ 0 & 0 & 0 & \kappa_{liq}^{\mathbb{Q}} \end{pmatrix} \left[ \begin{pmatrix} 0 \\ 0 \\ 0 \\ \theta_{liq}^{Q} \end{pmatrix} - \begin{pmatrix} L_t \\ S_t \\ C_t \\ X_t^{liq} \end{pmatrix} \right] dt + \Sigma \begin{pmatrix} dW_t^{L,\mathbb{Q}} \\ dW_t^{S,\mathbb{Q}} \\ dW_t^{C,\mathbb{Q}} \\ dW_t^{liq,\mathbb{Q}} \end{pmatrix},$$

where $\Sigma$ continues to be a diagonal matrix.

In the augmented AFNS-L model, inflation-indexed bonds are sensitive to bond-specific liquidity risks as the net present value of their future cash flow is calculated using the following discount function:

$$\overline{r}_t^i = r_t + \beta^i(1 - e^{-\lambda^{R,i}(t-t_0^i)})X_t^{liq} = L_t + S_t + \beta^i(1 - e^{-\lambda^{R,i}(t-t_0^i)})X_t^{liq}. \tag{4}$$

CR show that the net present value of one unit of consumption paid by BTU bond $i$ at time $t+\tau$ has the following exponential-affine form

$$\begin{aligned} P_t(t_0^i,\tau) &= E^{\mathbb{Q}}\Big[e^{-\int_t^{t+\tau}\overline{r}^i(s,t_0^i)ds}\Big] \\ &= \exp\Big(B_1(\tau)L_t + B_2(\tau)S_t + B_3(\tau)C_t + B_4(t,t_0^i,\tau)X_t^{liq} + A(t,t_0^i,\tau)\Big). \end{aligned}$$

This result implies that the model belongs to the class of Gaussian affine term structure models. Note also that, by fixing $\beta^i = 0$ for all $i$, we recover the AFNS model.

Now, consider the whole value of bond $i$ issued at time $t_0^i$ with maturity at $t+\tau^i$ that pays an annual coupon $C^i$ semiannually. Its price is given by[13]

$$\begin{aligned} P_t(t_0^i,\tau^i,C^i) &= C^i(t_1-t)E^{\mathbb{Q}}\Big[e^{-\int_t^{t_1}\overline{r}^{R,i}(s,t_0^i)ds}\Big] + \sum_{j=2}^{N}\frac{C^i}{2}E^{\mathbb{Q}}\Big[e^{-\int_t^{t_j}\overline{r}^{R,i}(s,t_0^i)ds}\Big] \\ &\quad + E^{\mathbb{Q}}\Big[e^{-\int_t^{t+\tau^i}\overline{r}^{R,i}(s,t_0^i)ds}\Big]. \end{aligned}$$

Unlike U.S. TIPS, Chilean inflation-indexed bonds have no embedded deflation protection option, which makes their pricing straightforward. There is only one minor omission in the bond pricing formula above. It does not account for the lag in the inflation indexation of the bond payoff. The potential error from this omission should be modest (see Grishchenko and Huang 2013), especially as we exclude bonds from our sample when they have less than one year remaining to maturity.

Finally, to complete the description of the AFNS-L model, we again specify an essentially affine risk premium structure, which implies that the risk premia $\Gamma_t$ take the form

$$\Gamma_t = \gamma^0 + \gamma^1 X_t,$$

where $\gamma^0 \in \mathbf{R}^4$ and $\gamma^1 \in \mathbf{R}^{4\times 4}$ contain unrestricted parameters. Thus, the resulting unrestricted four-factor AFNS-L model has $\mathbb{P}$-dynamics given by

$$\begin{pmatrix} dL_t \\ dS_t \\ dC_t \\ dX_t^{liq} \end{pmatrix} = \begin{pmatrix} \kappa_{11}^{\mathbb{P}} & \kappa_{12}^{\mathbb{P}} & \kappa_{13}^{\mathbb{P}} & \kappa_{14}^{\mathbb{P}} \\ \kappa_{21}^{\mathbb{P}} & \kappa_{22}^{\mathbb{P}} & \kappa_{23}^{\mathbb{P}} & \kappa_{24}^{\mathbb{P}} \\ \kappa_{31}^{\mathbb{P}} & \kappa_{32}^{\mathbb{P}} & \kappa_{33}^{\mathbb{P}} & \kappa_{34}^{\mathbb{P}} \\ \kappa_{41}^{\mathbb{P}} & \kappa_{42}^{\mathbb{P}} & \kappa_{43}^{\mathbb{P}} & \kappa_{44}^{\mathbb{P}} \end{pmatrix} \left( \begin{pmatrix} \theta_1^{\mathbb{P}} \\ \theta_2^{\mathbb{P}} \\ \theta_3^{\mathbb{P}} \\ \theta_4^{\mathbb{P}} \end{pmatrix} - \begin{pmatrix} L_t \\ S_t \\ C_t \\ X_t^{liq} \end{pmatrix} \right) dt + \Sigma \begin{pmatrix} dW_t^{L,\mathbb{P}} \\ dW_t^{S,\mathbb{P}} \\ dW_t^{C,\mathbb{P}} \\ dW_t^{liq,\mathbb{P}} \end{pmatrix}.$$

This is the transition equation in the Kalman filter estimation.

[13]This is the clean price that does not account for any accrued interest and maps to our observed bond prices.

### 3.3 Model Estimation and Econometric Identification

Due to the nonlinear relationship between the state variables and the bond prices, the model cannot be estimated with the standard Kalman filter. Instead, we use the extended Kalman filter as in Kim and Singleton (2012); see CR for details. Furthermore, to make the fitted errors comparable across bonds of various maturities, we scale each bond price by its duration. Thus, the measurement equation for the bond prices takes the following form

$$\frac{P_t^i(t_0^i, \tau^i)}{D_t^i(t_0^i, \tau^i)} = \frac{\widehat{P}_t^i(t_0^i, \tau^i)}{D_t^i(t_0^i, \tau^i)} + \varepsilon_t^i,$$

where $\widehat{P}_t^i(t_0^i, \tau^i)$ is the model-implied price of bond $i$ and $D_t^i(t_0^i, \tau^i)$ is its duration, which is calculated before estimation. See Andreasen et al. (2019) for evidence supporting this formulation of the measurement equation.

Furthermore, since the liquidity risk factor is a latent factor that we do not observe, its level is not identified without additional restrictions. As a consequence, we let the first 20-year inflation-indexed bond in our sample have a unit loading on this factor, that is, the 20-year inflation-indexed bond issued on September 11, 2002, and maturing on September 1, 2022, with 5 percent coupon has $\beta^i = 1$. This choice implies that the $\beta^i$ sensitivity parameters measure liquidity risk sensitivity relative to that of the 20-year 2022 bond.

Finally, we note that the $\lambda^{L,i}$ parameters can be hard to identify if their values are too large or too small. As a consequence, we follow ACR and impose the restriction that they fall within the range from 0.01 to 10, which is without practical consequences. Also, for numerical stability during model optimization, we impose the restriction that the $\beta^i$ parameters fall within the range from 0 to 100, which turns out not to be a binding constraint in optimum.

### 3.4 Estimation Results

This section presents our benchmark estimation results. In the interest of simplicity, in this section we focus on a version of the AFNS-L model where $K^{\mathbb{P}}$ and $\Sigma$ are diagonal matrices. As shown in ACR, these restrictions have hardly any effects on the estimated bond-specific liquidity risk premium for each inflation-indexed bond, because it is identified from the model's $\mathbb{Q}$-dynamics, which is independent of $K^{\mathbb{P}}$ and only display a weak link to $\Sigma$ through the small convexity adjustment in yields. Furthermore, we stress that we relax this assumption in Section 5 when we analyze estimates of $r_t^*$, which are indeed sensitive to the specification of the models' $\mathbb{P}$-dynamics.

Tables 4 and 5 report the summary statistics for the fitted errors of individual inflation-indexed bonds as well as for all bonds combined. With the two exceptions of bonds number 27 and 40 in our sample, there is otherwise uniform improvement in model fit from incorporating

| Inflation-indexed bond | Pricing errors | | | | Estimated parameters | | | |
|---|---|---|---|---|---|---|---|---|
| | AFNS | | AFNS-L | | AFNS-L | | | |
| | Mean | RMSE | Mean | RMSE | $\beta^i$ | SE | $\lambda^{L,i}$ | SE |
| (1) 5% 9/1/2007 | -1.92 | 9.82 | -0.64 | 5.20 | 1.1658 | 0.0475 | 9.9996 | 0.0686 |
| (2) 5% 9/1/2012 | 4.02 | 9.65 | 0.53 | 6.88 | 20.0931 | 0.0720 | 0.0100 | 0.0001 |
| (3) 5% 9/1/2022 | 0.15 | 6.96 | 0.12 | 5.27 | 1 | n.a. | 0.2170 | 0.0179 |
| (4) 5% 3/1/2008 | 1.14 | 6.22 | 0.98 | 5.71 | 1.6395 | 0.0571 | 0.4314 | 0.0422 |
| (5) 5% 9/1/2008 | 2.18 | 10.12 | 0.86 | 5.74 | 31.5122 | 0.0715 | 0.0126 | 0.0004 |
| (6) 4.5% 10/15/2023 | -1.26 | 8.47 | 0.18 | 6.87 | 0.9746 | 0.0111 | 0.2600 | 0.0294 |
| (7) 5% 11/1/2013 | 0.55 | 8.64 | 0.05 | 7.11 | 19.4150 | 0.0751 | 0.0100 | 0.0001 |
| (8) 4.5% 8/1/2024 | 2.01 | 12.97 | 0.18 | 7.00 | 1.0905 | 0.0176 | 0.1761 | 0.0171 |
| (9) 5% 9/1/2009 | 0.30 | 8.28 | 0.11 | 5.13 | 2.1811 | 0.0630 | 0.3732 | 0.0267 |
| (10) 5% 9/1/2010 | -1.08 | 9.14 | 0.00 | 8.03 | 2.0284 | 0.0520 | 0.4915 | 0.0391 |
| (11) 2.1% 9/1/2015 | -1.41 | 7.76 | 0.22 | 6.48 | 1.6451 | 0.0623 | 0.1956 | 0.0191 |
| (12) 2.6% 9/1/2025 | 1.05 | 7.11 | 0.38 | 5.89 | 1.3495 | 0.0560 | 0.1014 | 0.0119 |
| (13) 5% 1/1/2016 | -0.68 | 6.75 | 0.33 | 6.30 | 1.4326 | 0.0391 | 0.2933 | 0.0304 |
| (14) 5% 9/1/2011 | -3.31 | 17.35 | -0.86 | 9.43 | 1.7575 | 0.0254 | 0.9766 | 0.0581 |
| (15) 3% 3/1/2027 | 0.71 | 5.37 | 0.06 | 5.12 | 1.3258 | 0.0559 | 0.1264 | 0.0163 |
| (16) 3% 4/1/2012 | 4.03 | 9.98 | -0.37 | 8.05 | 2.2566 | 0.0581 | 0.4246 | 0.0293 |
| (17) 3% 5/1/2017 | -1.68 | 6.97 | 0.14 | 5.55 | 1.2658 | 0.0389 | 0.3368 | 0.0456 |
| (18) 3% 10/1/2012 | 1.58 | 10.70 | 0.59 | 8.06 | 1.9725 | 0.0504 | 0.5277 | 0.0399 |
| (19) 3% 1/1/2018 | -1.66 | 6.94 | -0.08 | 4.96 | 1.1805 | 0.0301 | 0.4011 | 0.0543 |
| (20) 3% 3/1/2028 | -0.58 | 5.84 | 0.07 | 5.25 | 1.3328 | 0.0560 | 0.1374 | 0.0189 |
| (21) 3% 3/1/2038 | 3.95 | 7.50 | 0.25 | 4.62 | 9.0822 | 0.0758 | 0.0101 | 0.0003 |
| (22) 3% 4/1/2013 | 5.33 | 12.92 | 0.40 | 7.93 | 2.6096 | 0.0710 | 0.2892 | 0.0171 |
| (23) 3% 5/1/2010 | 4.44 | 9.80 | 2.41 | 6.78 | 2.0772 | 0.0426 | 1.6507 | 0.0677 |
| (24) 3% 5/1/2028 | -1.04 | 6.35 | 0.04 | 5.88 | 1.3731 | 0.0535 | 0.1277 | 0.0154 |
| (25) 3% 7/1/2013 | 3.71 | 10.14 | 0.18 | 5.56 | 2.1879 | 0.0650 | 0.3966 | 0.0319 |
| (26) 3% 7/1/2018 | -1.36 | 6.32 | 0.21 | 4.18 | 1.1334 | 0.0358 | 0.4279 | 0.0621 |
| (27) 3% 8/1/2010 | -4.71 | 6.38 | 2.28 | 6.81 | 1.7147 | 0.0516 | 9.9997 | 0.0740 |
| (28) 3% 10/1/2013 | 2.30 | 9.02 | -0.04 | 5.29 | 1.8829 | 0.0486 | 0.5668 | 0.0521 |
| (29) 3% 10/1/2018 | -1.78 | 6.84 | 0.25 | 4.56 | 1.1058 | 0.0283 | 0.4457 | 0.0574 |
| (30) 3% 3/1/2029 | -0.42 | 7.28 | -0.41 | 5.69 | 1.4783 | 0.0596 | 0.1218 | 0.0138 |
| (31) 3% 3/1/2039 | 3.30 | 6.51 | 0.25 | 3.74 | 9.5306 | 0.0690 | 0.0101 | 0.0003 |
| (32) 3% 4/1/2014 | 1.99 | 13.92 | 0.31 | 10.61 | 1.5625 | 0.0208 | 10.0000 | 0.0687 |
| (33) 3% 5/1/2019 | -2.04 | 8.61 | -0.12 | 5.71 | 1.0548 | 0.0172 | 0.5185 | 0.0656 |
| (34) 3% 7/1/2014 | -0.20 | 11.78 | 0.09 | 7.52 | 1.5013 | 0.0239 | 10.0000 | 0.0751 |
| (35) 3% 7/1/2019 | -2.16 | 7.51 | 0.19 | 5.21 | 1.0300 | 0.0186 | 0.5865 | 0.0681 |
| (36) 3% 1/1/2015 | 1.35 | 8.56 | -0.31 | 7.41 | 1.4273 | 0.0203 | 10.0000 | 0.0687 |

Table 4: **Pricing Errors and Estimated Bond-Specific Risk Parameters**
This table reports the mean pricing errors (Mean) and the root mean-squared pricing errors (RMSE) of Chilean inflation-indexed bonds in the AFNS and AFNS-L models estimated with a diagonal specification of $K^{\mathbb{P}}$ and $\Sigma$. The errors are computed as the difference between the inflation-indexed bond market price expressed as yield to maturity and the corresponding model-implied yield. All errors are reported in basis points. Standard errors (SE) are not available (n.a.) for the normalized value of $\beta^3$.

| Inflation-indexed bond | Pricing errors | | | | Estimated parameters | | | |
|---|---|---|---|---|---|---|---|---|
| | AFNS | | AFNS-L | | AFNS-L | | | |
| | Mean | RMSE | Mean | RMSE | $\beta^i$ | SE | $\lambda^{L,i}$ | SE |
| (37) 3% 1/1/2020 | -2.03 | 7.65 | -0.06 | 5.02 | 1.0235 | 0.0209 | 0.5833 | 0.0672 |
| (38) 3% 1/1/2030 | -1.11 | 6.55 | -0.28 | 5.36 | 1.4138 | 0.0506 | 0.1549 | 0.0204 |
| (39) 3% 1/1/2040 | 2.77 | 4.88 | 0.17 | 3.44 | 10.0735 | 0.0708 | 0.0101 | 0.0003 |
| (40) 3% 7/1/2017 | 1.95 | 5.34 | -0.03 | 5.56 | 1.2334 | 0.0272 | 0.7716 | 0.0656 |
| (41) 3% 10/1/2015 | 0.70 | 6.32 | 0.26 | 5.20 | 1.3521 | 0.0200 | 1.5604 | 0.0730 |
| (42) 3% 2/1/2013 | -0.40 | 6.32 | 0.50 | 5.12 | 1.7910 | 0.0348 | 7.8633 | 0.0760 |
| (43) 3% 2/1/2016 | 2.32 | 6.98 | 0.00 | 4.87 | 1.3858 | 0.0236 | 1.0992 | 0.0710 |
| (44) 3% 2/1/2021 | 0.74 | 6.75 | 0.49 | 4.87 | 1.0708 | 0.0295 | 0.4295 | 0.0589 |
| (45) 3% 2/1/2031 | -1.92 | 6.50 | 0.10 | 4.97 | 1.4527 | 0.0564 | 0.1672 | 0.0237 |
| (46) 3% 2/1/2041 | 0.31 | 6.25 | 0.74 | 5.47 | 2.7158 | 0.0694 | 0.0579 | 0.0038 |
| (47) 3% 5/1/2013 | 1.71 | 5.78 | -0.09 | 5.07 | 1.7936 | 0.0382 | 9.9331 | 0.0778 |
| (48) 3% 8/1/2016 | 1.99 | 8.63 | 0.39 | 5.77 | 1.3037 | 0.0207 | 1.3756 | 0.0704 |
| (49) 3% 9/1/2013 | 1.77 | 6.84 | 0.11 | 3.81 | 1.7642 | 0.0443 | 10.0000 | 0.0744 |
| (50) 3% 1/1/2017 | -0.50 | 8.54 | -0.22 | 6.13 | 1.2263 | 0.0201 | 1.9934 | 0.0743 |
| (51) 3% 1/1/2019 | 1.60 | 5.95 | -0.03 | 4.45 | 1.0696 | 0.0209 | 2.7505 | 0.0713 |
| (52) 3% 1/1/2022 | 1.18 | 6.54 | 0.20 | 4.69 | 1.0262 | 0.0153 | 0.5880 | 0.0650 |
| (53) 3% 1/1/2032 | -1.65 | 5.66 | 0.36 | 4.46 | 1.5782 | 0.0590 | 0.1532 | 0.0188 |
| (54) 3% 1/1/2042 | 0.47 | 5.87 | 0.60 | 4.87 | 2.6262 | 0.0758 | 0.0682 | 0.0052 |
| (55) 3% 3/1/2017 | -0.23 | 6.87 | 0.08 | 4.62 | 1.2234 | 0.0246 | 1.6784 | 0.0719 |
| (56) 3% 3/1/2022 | 1.44 | 6.96 | -0.03 | 4.44 | 1.0440 | 0.0191 | 0.5105 | 0.0614 |
| (57) 3% 7/1/2017 | 0.86 | 6.03 | 0.09 | 5.40 | 1.2124 | 0.0247 | 1.6020 | 0.0720 |
| (58) 3% 3/1/2018 | 1.10 | 4.44 | 0.26 | 3.38 | 1.1396 | 0.0297 | 2.7592 | 0.0764 |
| (59) 3% 3/1/2023 | -2.43 | 7.87 | -0.09 | 5.37 | 0.9743 | 0.0157 | 0.9870 | 0.0735 |
| (60) 3% 8/1/2018 | 0.35 | 4.72 | 0.23 | 3.42 | 1.0918 | 0.0307 | 9.9451 | 0.0742 |
| (61) 3% 1/1/2024 | -0.13 | 11.71 | 0.35 | 8.63 | 0.9910 | 0.0098 | 1.8622 | 0.0714 |
| (62) 3% 1/1/2034 | -0.52 | 5.60 | 0.43 | 5.12 | 1.7945 | 0.0654 | 0.1552 | 0.0178 |
| (63) 3% 1/1/2044 | 3.02 | 6.46 | 0.62 | 4.49 | 2.8072 | 0.0782 | 0.0772 | 0.0064 |
| (64) 1.5% 3/1/2021 | 3.91 | 8.38 | -0.09 | 5.24 | 1.0562 | 0.0246 | 3.4525 | 0.0736 |
| (65) 1.5% 3/1/2026 | 2.39 | 8.07 | 0.39 | 5.68 | 1.1429 | 0.0192 | 0.8096 | 0.0756 |
| (66) 2% 3/1/2035 | -1.07 | 5.47 | 0.43 | 5.18 | 1.8297 | 0.0649 | 0.1813 | 0.0246 |
| (67) 1.3% 3/1/2023 | -4.00 | 10.31 | -0.74 | 6.04 | 1.0392 | 0.0260 | 0.8449 | 0.0780 |
| (68) 1.9% 9/1/2030 | -1.40 | 7.11 | 0.44 | 5.04 | 1.3089 | 0.0271 | 1.0722 | 0.0785 |
| (69) 2.1% 7/15/2050 | 5.21 | 10.12 | -0.04 | 6.17 | 3.2223 | 0.0825 | 0.1051 | 0.0111 |
| (70) 0% 3/1/2025 | -4.80 | 26.65 | 6.38 | 14.51 | 0.9941 | 0.0108 | 9.9999 | 0.0820 |
| (71) 0% 10/1/2028 | 3.01 | 10.30 | -0.96 | 6.33 | 1.2639 | 0.0375 | 9.9991 | 0.0922 |
| (72) 0% 10/1/2033 | 2.48 | 6.72 | 2.07 | 7.69 | 1.5288 | 0.0453 | 4.5830 | 0.0929 |
| All yields | 0.36 | 8.09 | 0.21 | 5.79 | - | - | - | - |
| Max $\mathcal{L}^{EKF}$ | 34,924.96 | | 36,559.58 | | - | | - | |

Table 5: **Pricing Errors and Estimated Bond-Specific Risk Parameters Cont.**
This table reports the mean pricing errors (Mean) and the root mean-squared pricing errors (RMSE) of Chilean inflation-indexed bonds in the AFNS and AFNS-L models estimated with a diagonal specification of $K^{\mathbb{P}}$ and $\Sigma$. The errors are computed as the difference between the inflation-indexed bond market price expressed as yield to maturity and the corresponding model-implied yield. All errors are reported in basis points. Standard errors (SE) are not available (n.a.) for the normalized value of $\beta^3$.

| Parameter | AFNS | | AFNS-L | |
|---|---|---|---|---|
| | Est. | SE | Est. | SE |
| $\kappa_{11}^{\mathbb{P}}$ | 0.0078 | 0.0075 | 0.0166 | 0.0417 |
| $\kappa_{22}^{\mathbb{P}}$ | 8.2822 | 0.0098 | 1.3911 | 0.0686 |
| $\kappa_{33}^{\mathbb{P}}$ | 1.5163 | 0.0094 | 0.5228 | 0.0674 |
| $\kappa_{44}^{\mathbb{P}}$ | - | - | 1.6283 | 0.0719 |
| $\sigma_{11}$ | 0.0032 | 0.0000 | 0.0066 | 0.0003 |
| $\sigma_{22}$ | 0.1000 | 0.0020 | 0.0323 | 0.0023 |
| $\sigma_{33}$ | 0.0341 | 0.0010 | 0.0310 | 0.0029 |
| $\sigma_{44}$ | - | - | 0.0734 | 0.0045 |
| $\theta_1^{\mathbb{P}}$ | 0.0874 | 0.0085 | 0.0575 | 0.0273 |
| $\theta_2^{\mathbb{P}}$ | -0.0527 | 0.0036 | -0.0314 | 0.0083 |
| $\theta_3^{\mathbb{P}}$ | -0.0394 | 0.0041 | -0.0225 | 0.0144 |
| $\theta_4^{\mathbb{P}}$ | - | - | 0.0170 | 0.0165 |
| $\lambda$ | 0.4232 | 0.0025 | 0.4082 | 0.0107 |
| $\kappa_{liq}^{\mathbb{Q}}$ | - | - | 3.3007 | 0.0682 |
| $\theta_{liq}^{\mathbb{Q}}$ | - | - | 0.0092 | 0.0004 |
| $\sigma_y$ | 0.0009 | $2.51 \times 10^{-6}$ | 0.0007 | $3.70 \times 10^{-6}$ |

Table 6: **Estimated Dynamic Parameters**
The table shows the estimated dynamic parameters for the AFNS and AFNS-L models estimated with a diagonal specification of $K^{\mathbb{P}}$ and $\Sigma$.

the bond-specific liquidity risk factor into the AFNS model. Still, it is worth noting that the AFNS model is able to deliver a root mean-squared fitted error of 8.1 basis points across all bonds combined, which in general could be characterized as a satisfactory fit, but obviously not as good as the RMSE of 5.8 basis points for all bonds combined achieved by the AFNS-L model, which represents a really good fit to the entire cross section of yields. Note also that neither 20- nor 30-year bonds pose any particular challenges for the two models. Thus, both the AFNS and AFNS-L models are clearly able to fit those long-term bond yields to a satisfactory level of accuracy.[14]

Table 6 contains the estimated dynamic parameters. With the exception of the slope factor, which is notably more persistent and less volatile in the AFNS-L model, the dynamics of the first three factors are qualitatively very similar across the two estimations. Furthermore, $\lambda$ is marginally smaller in the AFNS-L model. This implies that the yield loading of the slope factor decays toward zero at a slightly lower pace as maturity increases. At the same time, the peak of the curvature yield loadings is located at a later maturity. As a consequence, slope and curvature matter somewhat more for longer-term yields in the AFNS-L model.

The estimated paths of the level, slope, and curvature factors from the two models are shown in Figure 5. The two models' slope and curvature factors are fairly close to each

[14]See Christensen et al. (2022) for an analysis of such long-term bond yields.

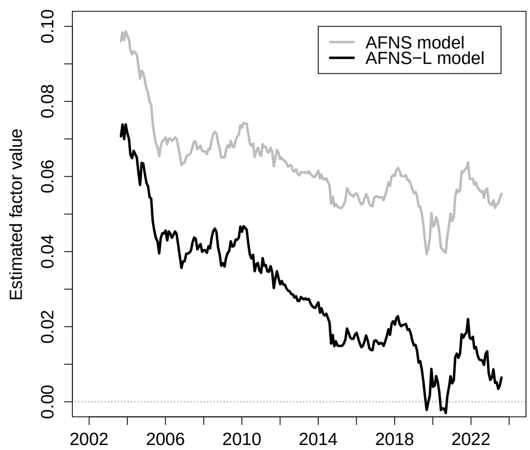


(a) $L_t$

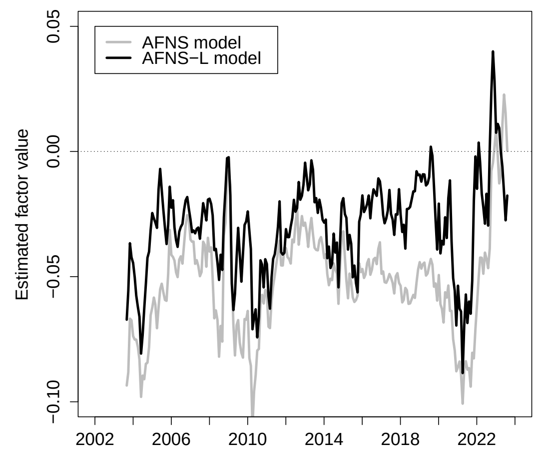


(b) $S_t$

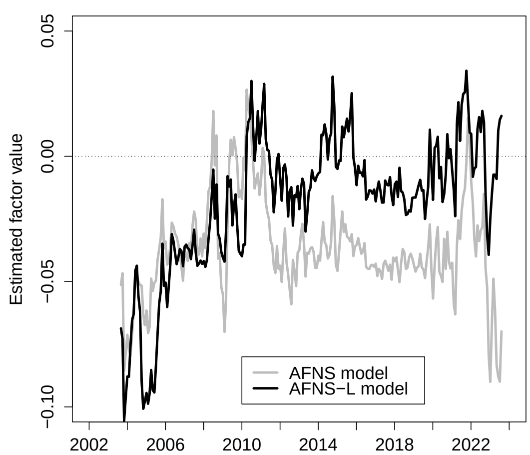


(c) $C_t$

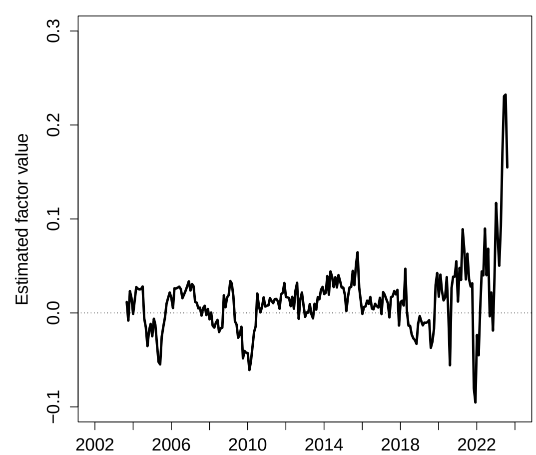


(d) $X_t^{liq}$

Figure 5: **Estimated State Variables**
Illustration of the estimated state variables from the AFNS and AFNS-L models.

other during the entire sample, while there is a notable persistent difference between the two estimated level factors. Accordingly, the main impact of accounting for bond-specific liquidity premia in the pricing of the inflation-indexed bonds is on the level of the frictionless real yield curve. The fourth factor in the AFNS-L model, the bond-specific liquidity risk factor, is a stationary quickly mean-reverting process without any pronounced persistent changes, although it did experience a large increase during the last year of the sample. Based on its historical pattern this outsized spike could be expected to be short-lived.

## 4 The Inflation-Indexed Bond Liquidity Premium

In this section, we analyze the inflation-indexed bond-specific liquidity premia implied by the estimated AFNS-L model described in the previous section. First, we formally define the bond-specific liquidity risk premia and study their historical evolution. We then assess the robustness of their estimation to various model and sample assumptions before we use regression analysis to examine their determinants.

### 4.1 The Estimated Inflation-Indexed Bond Liquidity Premium

We now use the estimated AFNS-L model to extract the liquidity premium in the Chilean inflation-indexed bond market. To compute this premium, we first use the estimated parameters and the filtered states $\{X_{t|t}\}_{t=1}^{T}$ to calculate the fitted inflation-indexed bond prices $\left\{\hat{P}_t^i\right\}_{t=1}^{T}$ for all outstanding securities in our sample. These bond prices are then converted into yields to maturity $\left\{\hat{y}_t^{c,i}\right\}_{t=1}^{T}$ by solving the fixed-point problem

$$\begin{aligned} \hat{P}_t^i &= C(t_1 - t)\exp\left\{-(t_1 - t)\hat{y}_t^{c,i}\right\} + \sum_{k=2}^{n} \frac{C}{2}\exp\left\{-(t_k - t)\hat{y}_t^{c,i}\right\} \\ &\quad + \exp\left\{-(T - t)\hat{y}_t^{c,i}\right\}, \end{aligned} \tag{5}$$

for $i = 1, 2, ..., n_t$, meaning that $\left\{\hat{y}_t^{c,i}\right\}_{t=1}^{T}$ is approximately the real rate of return on the $i$th bond if held until maturity (see Sack and Elsasser 2004). To obtain the corresponding yields with correction for the liquidity risk, we compute a new set of model-implied bond prices from the estimated AFNS-L model using only its frictionless part, i.e., using the constraints that $X_{t|t}^{liq} = 0$ for all $t$ as well as $\sigma_{44} = 0$ and $\theta_{liq}^{Q} = 0$. These prices are denoted $\left\{\tilde{P}_t^i\right\}_{t=1}^{T}$ and converted into yields to maturity $\tilde{y}_t^{c,i}$ using equation (5). They represent estimates of the prices that would prevail in a world without any financial frictions. The liquidity premium for the $i$th bond is then defined as

$$\Psi_t^i \equiv \hat{y}_t^{c,i} - \tilde{y}_t^{c,i}. \tag{6}$$

Figure 6 shows the average inflation-indexed bond liquidity premium $\bar{\Psi}_t$ across the outstanding bonds at each point in time. Although strictly positive as one could expect of a risk premium, the average estimated liquidity premium varies notably over time with a maximum of 303 basis points in summer 2023 and a low of 50 basis points in late 2021, when inflation had spiked to multidecade highs in Chile and much of the rest of the world. For the entire period it has an average of 111.73 basis points with a standard deviation of 31.09 basis points. Thus, liquidity premia represent a notable component in Chilean real yields as anticipated

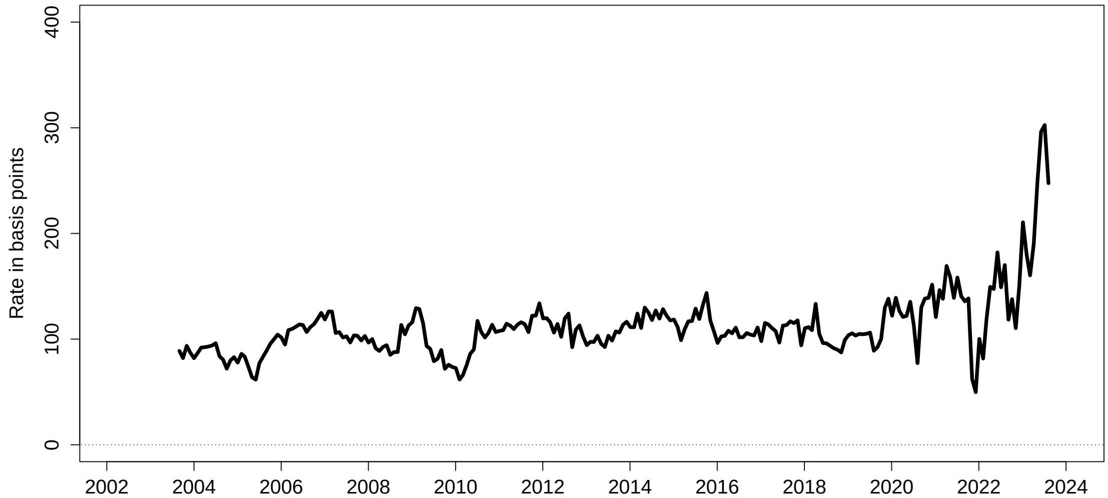


Figure 6: **Average Estimated Inflation-Indexed Bond Liquidity Premium**
Illustration of the average estimated inflation-indexed bond liquidity premium for each observation date implied by the AFNS-L model. The inflation-indexed bond liquidity premia are measured as the estimated yield difference between the fitted yield to maturity of individual inflation-indexed bonds and the corresponding frictionless yield to maturity with the liquidity risk factor turned off. The data cover the period from August 31, 2003, to July 31, 2023.

by the structural arguments laid out in Cardozo and Christensen (2023).

These results can be compared to those of ACR, who report that the average liquidity premium in U.S. TIPS is estimated at 34 basis points for the 1997-2013 period. The difference in liquidity premium levels across the TIPS and the Chilean inflation-indexed bond markets is likely to be due to the much greater relative liquidity of U.S. Treasury securities. Beauregard et al. (2023) report average estimated liquidity premia for Mexican inflation-indexed bonds, also known as udibonos, around 47 basis points during the 2009-2019 period. In contrast, Cardozo and Christensen (2023) report estimated liquidity premia for Colombian inflation-indexed bonds, so-called bonos UVR, that average 225 basis points with a standard deviation of 32 basis points during the 2005-2020 period. Overall, we take these results to imply that our estimated liquidity premia for Chilean inflation-indexed bonds are of reasonable size and fall within the range of estimates reported for other comparable markets of inflation-indexed bonds.

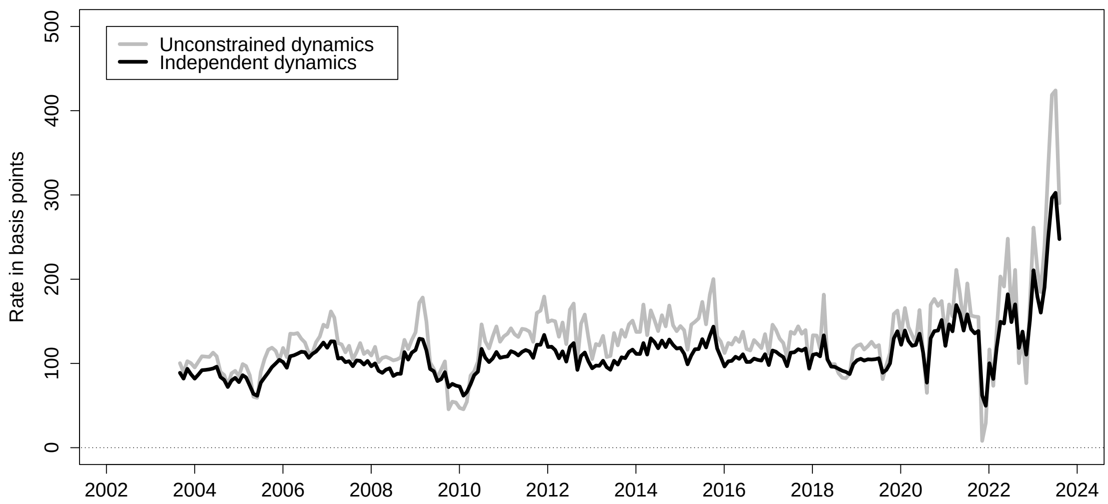


Figure 7: **Average Estimated Inflation-Indexed Bond Liquidity Premium: Alternative $\mathbb{P}$ Dynamics**
Illustration of the average estimated inflation-indexed bond liquidity premium for each observation date implied by the AFNS-L model when estimated with unconstrained dynamics as detailed in the text instead of independent factor dynamics. In both cases, the inflation-indexed bond liquidity premia are measured as the estimated yield difference between the fitted yield to maturity of individual inflation-indexed bonds and the corresponding frictionless yield to maturity with the liquidity risk factor turned off.

## 4.2 Robustness Analysis

This section examines the robustness of the average liquidity premium reported in the previous section to some of the main assumptions imposed so far. Throughout the section, the AFNS-L model with diagonal $K^{\mathbb{P}}$ and $\Sigma$ matrices serves as the benchmark for the reasons already listed in Section 3.4.

First, we assess whether the specification of the dynamics within the AFNS-L model matters for the estimated Chilean inflation-indexed bond liquidity premium. To do so, we estimate the AFNS-L model with unconstrained dynamics, that is, the AFNS-L model with unrestricted $K^{\mathbb{P}}$ and lower triangular $\Sigma$ matrix. Figure 7 shows the estimated inflation-indexed liquidity premium from this estimation and compares it to the series produced by our benchmark model. Note that they are highly positively correlated and only marginally higher in the unconstrained model. Thus, we conclude that the specification of the dynamics within the AFNS-L model plays only a modest role for the estimated bond-specific liquidity risk premia, which is consistent with the findings of ACR in the context of U.S. TIPS.

Second, we assess whether the data frequency plays any role for our results. To do so,

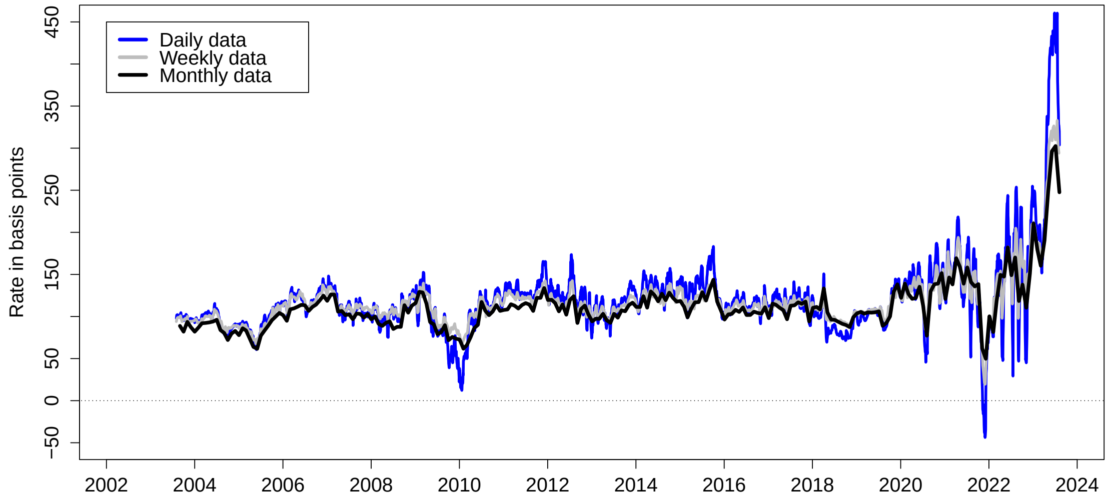


Figure 8: **Average Estimated Inflation-Indexed Bond Liquidity Premium: Data Frequency**
Illustration of the average estimated inflation-indexed bond liquidity premium for each observation date implied by the AFNS-L model when estimated using daily, weekly, and monthly data. In both cases, the inflation-indexed bond liquidity premia are measured as the estimated yield difference between the fitted yield to maturity of individual inflation-indexed bonds and the corresponding frictionless yield to maturity with the liquidity risk factor turned off.

we estimate the AFNS-L model using daily, weekly, and monthly data; based on the results above, it suffices to focus on the most parsimonious AFNS-L model with diagonal $K^{\mathbb{P}}$ and $\Sigma$ matrices. Figure 8 shows the estimated inflation-indexed bond liquidity premium series from the three estimations. Note that they are all very close to each other. Thus, we conclude that data frequency matters little for our results. Clearly, at the higher daily and weekly frequencies, there are some isolated sharp spikes that are absent in the monthly series, but they are too infrequent and short-lived to have an impact on the estimation results.

## 4.3 Regression Analysis

In this section, we use regression analysis to find the key determining factors driving the variation in the average estimated inflation-indexed bond liquidity premium series. To explain its variation, we run a battery of standard regressions with it as the dependent variable and a wide set of explanatory variables that are thought to play a role for liquidity risk premia as explained in the following.

First, it seems intuitive that the size of the inflation-indexed bond market should matter for the liquidity risk premium investors demand for holding inflation-indexed bonds. To test this conjecture, we use the monthly total outstanding amount of inflation-indexed bonds scaled by nominal GDP.

Our second key explanatory variable is motivated by the structural arguments in Cardozo and Christensen (2023), which suggest that holdings of inflation-indexed bonds should be tilted towards domestic patient buy-and-hold investors. To test that hypothesis, we include the pension fund share defined as Chilean pension fund holdings of inflation-indexed bonds divided by the total outstanding amount of inflation-indexed bonds. We consider this a proxy for the holdings of all domestic buy-and-hold investors in Chile. Our conjecture is that a higher concentration of market share among such investors should increase the liquidity risk of the indexed bonds as it becomes harder for investors to sell them back to the market if hit with an unexpected liquidity shock. This should make investors demand a higher liquidity premium for assuming the higher risk, all else being equal.

In Table 7, column (1) reports the result of using these two variables to explain the variation in the average estimated inflation-indexed liquidity premium series. We note that we get a significant negative coefficient on the indexed BTU market-to-GDP ratio. This means that an expansion of the inflation-indexed bond market relative to GDP tends to put downward pressure on inflation-indexed bond liquidity premia—a positive effect of increased supply. At the same time, we get a significant positive coefficient on the pension fund share confirming our conjecture and that of Christensen and Cardozo (2023), that is, as the market becomes more dominated by buy-and-hold investors, its steady state moves towards one of increasing liquidity premia. Hence, positive effects from an expansion of the market relative to the size of the economy may be offset provided the extra bond volume is acquired by domestic buy-and-hold investors.

To verify the robustness of these findings, we next consider several groups of control variables.

To begin, we are interested in the role of factors that are believed to matter for inflation-indexed bond market liquidity specifically. First, we use the average bid-ask spread in the inflation-indexed bond market shown in Figure 4. Second, we add the average inflation-indexed bond age and the one-month realized volatility of the ten-year inflation-indexed bond yield as additional proxies for bond liquidity following the work of Houweling et al. (2005). Inspired by the analysis of Hu et al. (2013), we also include a noise measure of the bond prices to control for variation in the amount of arbitrage capital available in this market. Lastly, we include the inflation-indexed bond market turnover measured as the monthly inflation-indexed bond transaction volume divided by the total outstanding amount of inflation-indexed bonds. Adding these five control variables tied to bond market liquidity and functioning produces the results reported in regression (2) in Table 7. We note an increase in the adjusted $R^2$ to 0.32. However, the control variables are all insignificant except for the average bond age variable, while our two key explanatory variables preserve their statistically significant coefficients, even though they are somewhat smaller in size.

After having explored the role of liquidity factors, we examine the effects of factors reflecting risk sentiment domestically and globally on the inflation-indexed liquidity premium series. This set of variables includes the VIX, which represents near-term uncertainty about the general stock market as reflected in options on the Standard & Poor's 500 stock price index and is widely used as a gauge of investor fear and risk aversion. We also control for a measure of financial frictions in the U.S. Treasury market, the so-called on-the-run (OTR) premium, which captures the difference between seasoned (off-the-run) U.S. Treasury securities and the most recently issued (on-the-run) U.S. Treasury security of the same 10-year maturity. To control for factors that affect emerging market sovereign bonds more broadly, we include the J.P. Morgan Emerging Market Bond Index (EMBI). As an additional indicator of credit risk and credit risk sentiment, we use the five-year credit default swap (CDS) rate for Chile. This set also includes the MOVE index, which is a representative measure of the implied volatility in the U.S. Treasury market and hence serves as a proxy for the risk of fixed-income investments broadly defined. The results of the regression with these five added control variables are reported in regression (3) in Table 7. We note an increase in the adjusted $R^2$ to 0.38. Still, only the OTR premium and MOVE have a significant coefficient, and the former even has a negative sign. More importantly, our two key explanatory variables preserve their significant coefficients as in the original regression.

In the final group, we assess the role played by standard macro variables for the inflation-indexed liquidity risk premium series. First, to capture inflation risk in a direct way, we include the year-over-year change in the Chilean CPI. Second, we consider the role of political uncertainty by including a measure of economic policy uncertainty (EPU) in Chile.[15] Next, we include the Chilean monetary policy rate. In addition to capturing the stance of monetary policy, this rate may serve as a proxy for the opportunity cost of holding money and the associated liquidity convenience premia of inflation-indexed bonds, as explained in Nagel (2016). The final variable in the set is a measure of relative prices of traded goods for the Chilean economy, which are proxied by the log ratio of copper prices over the West Texas Intermediate (WTI) Cushing crude oil price. The results of the regression with these four standard macroeconomic control variables are reported in regression (4) in Table 7. It produces a high adjusted $R^2$ of 0.45. However, none of the macroeconomic variables are statistically significant. Still, our two key explanatory variables remain statistically significant.

To assess the robustness of the results from the first four regressions, we include all variables with the results reported in column (5) in the table. Although this joint regression produces a high adjusted $R^2$ of 0.49, none of the control variables are statistically significant

[15] This is taken from https://www.policyuncertainty.com/chile_monthly.html

| Explanatory variables | (1) | (2) | (3) | (4) | (5) |
|---|---|---|---|---|---|
| BTU market-to-GDP ratio | -16.47*** | -9.05** | -15.64*** | -12.38*** | -8.96** |
| | (5.63) | (3.96) | (5.02) | (4.22) | (3.72) |
| Pension fund share | 4.74*** | 2.35* | 4.16*** | 3.08*** | 3.08*** |
| | (1.45) | (1.25) | (1.10) | (0.98) | (0.99) |
| Bid-ask spread | | 3.03 | | | -2.45 |
| | | (2.03) | | | (1.63) |
| Avg. bonos age | | 3.14* | | | 2.70 |
| | | (1.62) | | | (2.53) |
| One-month bond vol. | | -0.56 | | | -1.04* |
| | | (0.69) | | | (0.53) |
| Noise measure | | 2.14 | | | 2.78 |
| | | (3.42) | | | (2.39) |
| Turnover | | -0.71 | | | 0.63 |
| | | (0.54) | | | (0.52) |
| VIX | | | -0.52 | | -0.21 |
| | | | (0.57) | | (0.40) |
| OTR premium | | | -2.49*** | | -0.17 |
| | | | (0.80) | | (0.77) |
| EMBI | | | -0.09 | | -0.17 |
| | | | (0.10) | | (0.14) |
| CDS rate | | | 0.13 | | 0.13 |
| | | | (0.22) | | (0.30) |
| MOVE | | | 0.76** | | 0.25 |
| | | | (0.36) | | (0.24) |
| CPI Inflation | | | | 0.32 | 0.40 |
| | | | | (3.80) | (2.71) |
| EPU Chile | | | | 0.04 | 0.07 |
| | | | | (0.07) | (0.06) |
| Monetary policy rate | | | | 5.84 | 4.30 |
| | | | | (4.92) | (3.49) |
| Relative prices | | | | 9.91 | 14.51 |
| | | | | (12.35) | (13.66) |
| Intercept | -21.35 | 23.33 | -24.60 | 47.95 | 11.05 |
| | (39.04) | (66.82) | (32.43) | (52.68) | (66.83) |
| Adjusted $R^2$ | 0.20 | 0.32 | 0.38 | 0.45 | 0.49 |

Table 7: **Regression Results for the Average Estimated Inflation-Indexed Bond Liquidity Premium**

The table reports the results of regressions with the average estimated inflation-indexed bond liquidity risk premium as the dependent variable and 16 explanatory variables. Standard errors computed by the Newey-West estimator (with three lags) are reported in parentheses. Asterisks *, ** and *** indicate significance at the 10 percent, 5 percent and 1 percent levels, respectively.

at the 5 percent level. More importantly, our two key explanatory variables remain statistically significant and preserve both their sign and approximate magnitudes as in the earlier regressions. As a consequence, we consider our findings to be robust.

Related to our findings we note that the presence of large institutional investors and their influence on domestic markets have been extensively documented as pivotal drivers of liquidity and risk premia; see Pritsker (2002) and Vayanos and Vila (2021), among many others. In the context of Chile, the main investors in the domestic government fixed-income markets are so-called pension fund administrators. As of June 2023, this group of investors held nearly 70 percent of the total stock of BTUs. The strong significance of the coefficient on their market share in our regressions is likely to be explained by the buy-and-hold investment approach followed by these funds, along with their preference for longer-maturity bonds. Furthermore, we evaluate the impact of the size of the domestic bond market—proxied by the total outstanding bonds relative to GDP—on the bond liquidity premium. Following the onset of the COVID-19 pandemic, there has been a reduction in the magnitude of the domestic bond market, declining from 13 percent of GDP in the 2013-2019 period to 10 percent of GDP in the post-pandemic era. During the same period, there are matching reductions in the proxies of bond liquidity such as market bond turnover and an increase in bid-ask spreads.

In terms of the interpretation of the estimated coefficients, our results have the following implications: An increase of 1 percentage point in the pension fund market share is correlated with an increase of about 3 basis points in our bond liquidity premium series. In contrast, an increase of 1 percentage point in the BTU market size is correlated with a reduction in the bond liquidity premium of around 9 basis points. Thus, the overall size of the market seems to matter more than the distribution of the market shares, or put differently, the negative impact on BTU market liquidity from an increase in investor concentration can be overcome through an increase in the market size, in particular if the new issuance is acquired by investors pursuing active trading strategies such as hedge funds or foreign investors even though we admit that this is a challenging outcome to achieve given the intrinsic dynamics in this market.

## 5 A New Normal for Chilean Interest Rates?

In this section, we first introduce our market-based definition of the natural real rate before we go through a careful model selection process to find a preferred specification of the AFNS-L model's objective $\mathbb{P}$-dynamics. We then use this AFNS-L model to account for liquidity and term premia in the inflation-indexed bond prices and obtain expected real short rates and the associated measure of the equilibrium real rate. Finally, we compare this estimate to other market-based and macro-based estimates from the literature and consider the persistence of forces that may be pushing the real rate lower in Chile.

### 5.1 Definition of the Natural Rate

Our working definition of the equilibrium real rate of interest $r_t^*$ is

$$r_t^* = \frac{1}{5}\int_{t+5}^{t+10} E_t^{\mathbb{P}}[r_s^R]ds, \tag{7}$$

that is, the average expected real short rate over a five-year period starting five years ahead where the expectation is with respect to the objective $\mathbb{P}$-probability measure. As explained in CR, this 5yr5yr forward average expected real short rate should be little affected by short-term transitory shocks. Alternatively, $r_t^*$ could be defined as the expected real short rate at an infinite horizon. However, this quantity will depend crucially on whether the factor dynamics exhibit a unit root. As is well known, the typical spans of time series data that are available do not distinguish strongly between highly persistent stationary processes and nonstationary ones. Our model follows the finance literature and adopts the former structure, so strictly speaking, our infinite-horizon steady-state expected real rate is constant. However, we do not view our data sample as having sufficient information in the 10-year to infinite horizon range to definitively pin down that steady state, so we prefer our definition with a medium- to long-run horizon.

### 5.2 Model Selection

For estimation of the natural real rate and associated real term premia, the specification of the mean-reversion matrix $K^{\mathbb{P}}$ is critical, as noted earlier. To select the best fitting specification of the model's real-world dynamics, we use a general-to-specific modeling strategy in which the least significant off-diagonal parameter of $K^{\mathbb{P}}$ is restricted to zero and the model is re-estimated. This strategy of eliminating the least significant coefficient starts from the AFNS-L model with an unrestricted $K^{\mathbb{P}}$ matrix and is carried out down to the most parsimonious specification, which has a diagonal $K^{\mathbb{P}}$ matrix. The final specification choice is based on the value of the Bayesian information criterion (BIC), as in Christensen et al. (2014).[16]

The summary statistics of the model selection process are reported in Table 8. The BIC

[16]The Bayesian information criterion is defined as $\text{BIC} = -2\log L + k\log T$, where $k$ is the number of model parameters and $T = 240$ is the number of monthly data observations.

| Alternative specifications | Goodness of fit statistics | | | |
|---|---|---|---|---|
| | $\log L$ | $k$ | $p$-value | BIC |
| (1) Unrestricted $K^{\mathbb{P}}$ | 36,592.74 | 171 | n.a. | -72,248.29 |
| (2) $\kappa^{\mathbb{P}}_{23} = 0$ | 36,592.74 | 170 | 1.00 | -72,253.77 |
| (3) $\kappa^{\mathbb{P}}_{23} = \kappa^{\mathbb{P}}_{14} = 0$ | 36,592.66 | 169 | 0.69 | -72,259.09 |
| (4) $\kappa^{\mathbb{P}}_{23} = \kappa^{\mathbb{P}}_{14} = \kappa^{\mathbb{P}}_{13} = 0$ | 36,591.06 | 168 | 0.07 | -72,261.37 |
| (5) $\kappa^{\mathbb{P}}_{23} = \ldots = \kappa^{\mathbb{P}}_{34} = 0$ | 36,590.40 | 167 | 0.25 | -72,265.53 |
| (6) $\kappa^{\mathbb{P}}_{23} = \ldots = \kappa^{\mathbb{P}}_{42} = 0$ | 36,590.04 | 166 | 0.40 | -72,270.29 |
| (7) $\kappa^{\mathbb{P}}_{23} = \ldots = \kappa^{\mathbb{P}}_{24} = 0$ | 36,585.05 | 165 | $< 0.01$ | -72,265.79 |
| (8) $\kappa^{\mathbb{P}}_{23} = \ldots = \kappa^{\mathbb{P}}_{21} = 0$ | 36,583.15 | 164 | 0.05 | -72,267.48 |
| (9) $\kappa^{\mathbb{P}}_{23} = \ldots = \kappa^{\mathbb{P}}_{43} = 0$ | 36,582.26 | 163 | 0.18 | -72,271.18 |
| (10) $\kappa^{\mathbb{P}}_{23} = \ldots = \kappa^{\mathbb{P}}_{41} = 0$ | 36,579.90 | 162 | 0.03 | **-72,271.94** |
| (11) $\kappa^{\mathbb{P}}_{23} = \ldots = \kappa^{\mathbb{P}}_{12} = 0$ | 36,572.27 | 161 | $< 0.01$ | -72,262.16 |
| (12) $\kappa^{\mathbb{P}}_{23} = \ldots = \kappa^{\mathbb{P}}_{32} = 0$ | 36,564.98 | 160 | $< 0.01$ | -72,253.06 |
| (13) $\kappa^{\mathbb{P}}_{23} = \ldots = \kappa^{\mathbb{P}}_{31} = 0$ | 36,559.58 | 159 | $< 0.01$ | -72,247.74 |

Table 8: **Evaluation of Alternative Specifications of the AFNS-L Model**
There are thirteen alternative estimated specifications of the AFNS-L model. Each specification is listed with its maximum log likelihood ($\log L$), number of parameters ($k$), the $p$-value from a likelihood ratio test of the hypothesis that it differs from the specification above with one more free parameter, and the Bayesian information criterion (BIC). The period analyzed covers monthly data from August 31, 2003, to July 31, 2023.

is minimized by specification (10), which has a $K^{\mathbb{P}}$ matrix given by

$$K^{\mathbb{P}}_{BIC} = \begin{pmatrix} \kappa^{\mathbb{P}}_{11} & \kappa^{\mathbb{P}}_{12} & 0 & 0 \\ 0 & \kappa^{\mathbb{P}}_{22} & 0 & 0 \\ \kappa^{\mathbb{P}}_{31} & \kappa^{\mathbb{P}}_{32} & \kappa^{\mathbb{P}}_{33} & 0 \\ 0 & 0 & 0 & \kappa^{\mathbb{P}}_{44} \end{pmatrix}.$$

The estimated parameters of the preferred specification are reported in Table 9. The estimated $\mathbb{Q}$-dynamics used for pricing and determined by ($\Sigma$, $\lambda$, $\kappa^{\mathbb{Q}}_{liq}$, $\theta^{\mathbb{Q}}_{liq}$) are very close to those reported in Table 6 for the AFNS-L model with diagonal $K^{\mathbb{P}}$. This implies that both model fit and the estimated inflation-indexed bond liquidity premia from the preferred AFNS-L model are very similar to those already reported and therefore not shown. Furthermore, the estimated objective $\mathbb{P}$-dynamics in terms of $\theta^{\mathbb{P}}$ and $\Sigma$ are also qualitatively similar to those reported in Table 6. Finally, there are intriguing significant dynamic interactions between the level, slope, and curvature factors in our preferred specification. To understand the role played by the mean-reversion matrix $K^{\mathbb{P}}$ for estimates of the natural real rate, we will later analyze the most flexible model with unrestricted mean-reversion matrix $K^{\mathbb{P}}$ and the most parsimonious model with diagonal $K^{\mathbb{P}}$ in addition to our preferred specification described above.

| $K^{\mathbb{P}}$ | $K^{\mathbb{P}}_{\cdot,1}$ | $K^{\mathbb{P}}_{\cdot,2}$ | $K^{\mathbb{P}}_{\cdot,3}$ | $K^{\mathbb{P}}_{\cdot,4}$ | $\theta^{\mathbb{P}}$ | | $\Sigma$ |
|---|---|---|---|---|---|---|---|
| $K^{\mathbb{P}}_{1,\cdot}$ | 0.2745 | 0.4016 | 0 | 0 | 0.0607 | $\sigma_{11}$ | 0.0064 |
| | (0.0546) | (0.0518) | | | (0.0146) | | (0.0003) |
| $K^{\mathbb{P}}_{2,\cdot}$ | 0 | 0.4613 | 0 | 0 | -0.0591 | $\sigma_{22}$ | 0.0316 |
| | | (0.0670) | | | (0.0128) | | (0.0023) |
| $K^{\mathbb{P}}_{3,\cdot}$ | 3.9204 | 2.0614 | 2.5954 | 0 | -0.0441 | $\sigma_{33}$ | 0.0321 |
| | (0.0657) | (0.0663) | (0.0656) | | (0.0154) | | (0.0024) |
| $K^{\mathbb{P}}_{4,\cdot}$ | 0 | 0 | 0 | 1.6384 | 0.0166 | $\sigma_{44}$ | 0.0734 |
| | | | | (0.0674) | (0.0152) | | (0.0045) |

Table 9: **Estimated Dynamic Parameters of the Preferred AFNS-L Model**
The table shows the estimated parameters of the $K^{\mathbb{P}}$ matrix, $\theta^{\mathbb{P}}$ vector, and diagonal $\Sigma$ matrix for the preferred AFNS-L model according to the BIC. The estimated value of $\lambda$ is 0.3955 (0.0095), while $\kappa^{\mathbb{Q}}_{liq} = 3.2534$ (0.0677), and $\theta^{\mathbb{Q}}_{liq} = 0.0096$ (0.0004). The maximum log likelihood value is 36,579.90. The numbers in parentheses are the estimated parameter standard deviations.

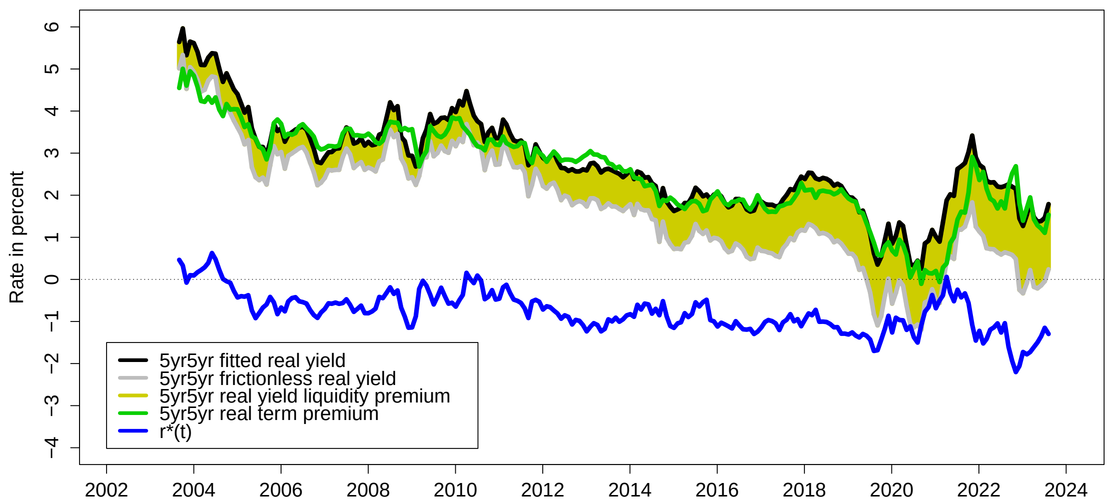


Figure 9: **AFNS-L Model 5yr5yr Real Yield Decomposition**

## 5.3 Estimates of the Natural Rate

Our market-based measure of the natural rate is the average expected real short rate over a five-year period starting five years ahead. This 5yr5yr forward average expected real short rate should be little affected by short-term transitory shocks and well positioned to capture the persistent trends in the natural real rate.

To illustrate the decomposition underlying our definition of $r^*_t$, recall that the real term premium is defined as

$$TP_t(\tau) = y_t(\tau) - \frac{1}{\tau}\int_t^{t+\tau} E_t^{\mathbb{P}}[r_s]ds.$$

That is, the real term premium is the difference in expected real return between a buy-and-hold strategy for a $\tau$-year real bond and an instantaneous rollover strategy at the risk-free real rate $r_t$. Figure 9 shows the AFNS-L model decomposition of the 5yr5yr forward frictionless real yield based on this equation. The solid green line is the 5yr5yr forward real term premium, which, although volatile, has fluctuated around a fairly stable level since the early 2000s. Although theory suggests that this premium is countercyclical and elevated during economic recessions, our estimates only partially align with these characteristics. In contrast, the estimate of the natural rate of interest implied by the AFNS-L model—the blue line—shows a gradual decline from around 0.5 percent in the early 2000s to below -2 percent by mid-2022. Importantly, it has remained low since then despite the recent large increases in bond yields. By the end of our sample, the estimate of $r_t^*$ stands at -1.30 percent.

Equally important, note the sizable inflation-indexed bond liquidity premia that drive a large wedge between the observed 5yr5yr real yield shown with a solid black line and the lower 5yr5yr frictionless real yield shown with a solid gray line. Thus, without the liquidity premium adjustment, one might be led to believe that real yields are much higher than what is actually the case, a point also made by Andreasen and Christensen (2016) in the context of U.S. TIPS.

### 5.3.1 Sensitivity Analysis

To assess the sensitivity of our $r_t^*$ estimate to the specification of the mean-reversion matrix $K^{\mathbb{P}}$, we compare it in Figure 10 to the estimates from the AFNS-L models with unrestricted and diagonal $K^{\mathbb{P}}$ matrix, respectively. As can be seen from the figure, our $r_t^*$ estimate is indeed somewhat sensitive to this model choice, but flexible specifications like our preferred AFNS-L model specification tend to give fairly similar $r_t^*$ estimates. Note also that all three estimates are dominated by a persistent lower trend during the entire 20-year sample period.

The role of the data frequency is examined in Figure 11, which shows the $r_t^*$ estimates implied by our preferred AFNS-R model estimated at daily, weekly, and monthly frequency. The results show that our estimate has little sensitivity to our choice to focus on conventional monthly data to facilitate model estimation. However, these results demonstrate that it would be possible to use our model for high-frequency daily policy and market monitoring analysis.

## 5.4 Comparison of Estimates of the Natural Rate

In this section, we compare our estimate of the natural real rate to other existing estimates of the equilibrium or natural interest rate in the literature. To start, we compare the $r_t^*$ estimate

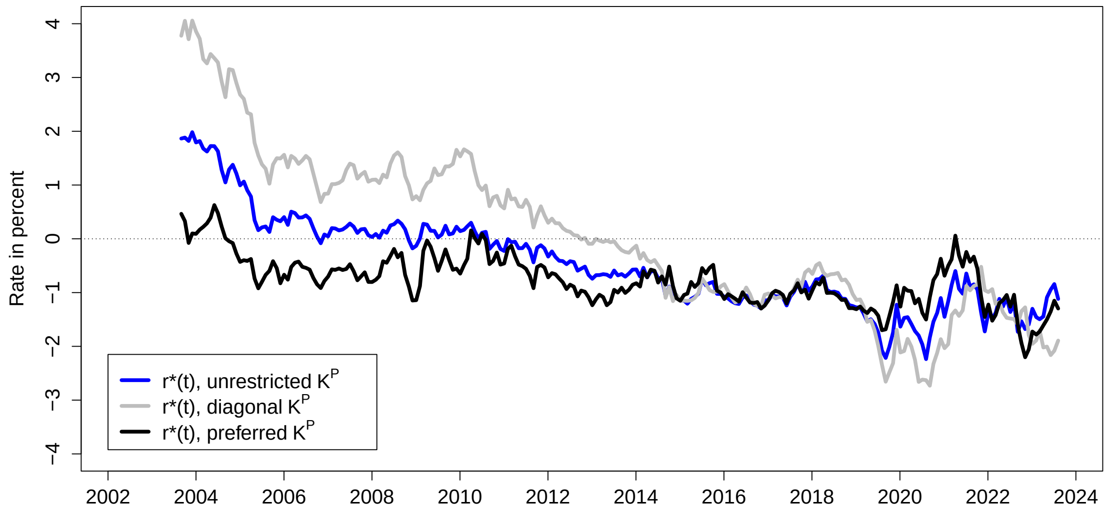


Figure 10: **The Sensitivity of r$^*$ Estimates to $K^{\mathbb{P}}$ Specification**

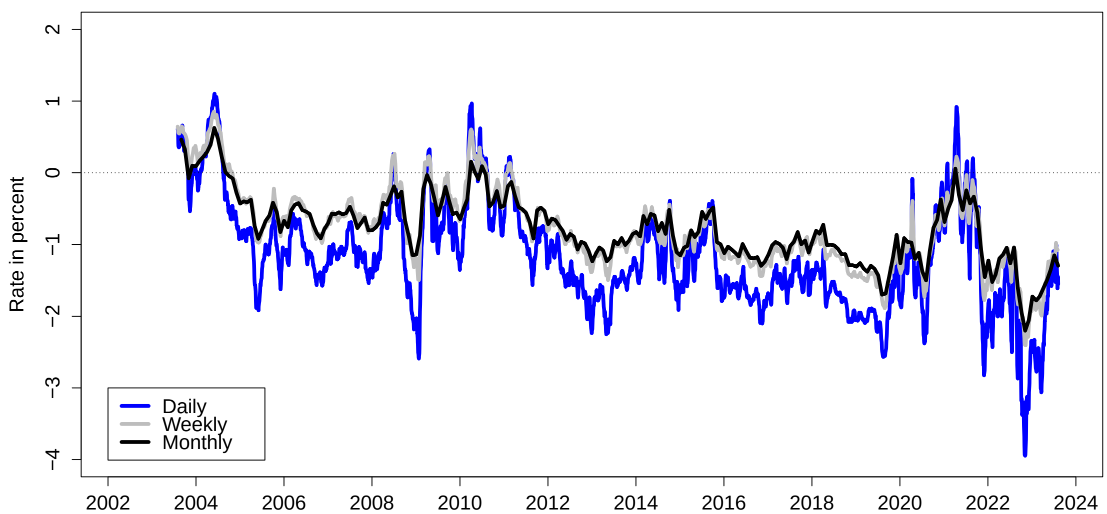


Figure 11: **The Sensitivity of r$^*$ Estimates to Data Frequency**

from the AFNS-L model to the Mexican market-based estimate reported by Beauregard et al. (2023, henceforth BCFZ) using a combination of Mexican nominal bond prices and prices of Mexican inflation-indexed bonds, so-called udibonos, and to a similar Colombian market-based estimate calculated from an update of the analysis in Cardozo and Christensen (2023,

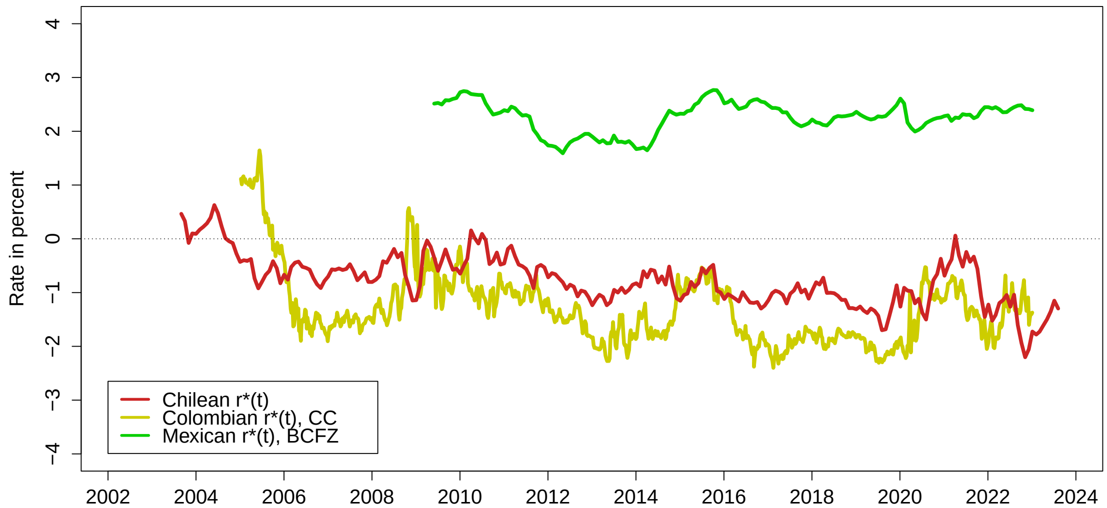


Figure 12: **Comparison with Foreign Market-Based Estimates of r$^*$**

henceforth CC). These three market-based estimates of the natural real rate are shown in Figure 12. The high positive correlation and similar downward trend between the Chilean and Colombian estimates are both evident. In contrast, the Mexican estimate has remained stable and fluctuated around 2.5 percent over the past decade. Importantly, none of the estimates have been materially affected by the COVID-19 pandemic or its aftermath. Similarly, the Global Financial Crisis of 2008-2009 also appears to have left at most modest prints on the $r_t^*$ estimates. Hence, they share the common feature that their most pronounced declines over the past two decades happened before and after, but *not* during the Global Financial Crisis.

Now, we turn to the crucial comparison of our finance-based estimate of $r_t^*$ with an estimate based on macroeconomic data. Figure 13 shows the $r_t^*$ estimate from our preferred AFNS-L model along with the macro-based estimate of $r^*$ from a staff implementation of the Holston et al. (2017, henceforth HLW) model using Chilean macro data.[17] The macro-based estimate shown in the figure starts in 1988 before our yield data. Importantly, both series are characterized by persistent secular declines. For the overlapping period between 2003 and 2022, we note that the macro-based estimate is more volatile and assumes both the highest and the lowest values. Hence, our finance-based $r_t^*$ estimate is entirely within the range of the macro-based estimate. Overall, we consider this evidence favorable to our yields-only approach to estimating $r_t^*$.

[17] This is the filtered estimate generated by applying the approach described in Laubach and Williams (2003) to Chilean macroeconomic series.


Figure 13: **Comparison with a Macro-Based Estimate of r***

## 5.5 Projections of the Natural Rate

In light of the intense debate among researchers, investors, and policymakers about whether there is a new higher normal for interest rates, we end our analysis by presenting the outlook for the natural real rate based on the preferred AFNS-L model. We follow the approach of Christensen et al. (2015) and simulate 10,000 factor paths over a ten-year horizon conditioned on the shape of the inflation-indexed yield curve and investors' embedded forward-looking expectations as of the end of our sample (that is, using estimated state variables and factor dynamics as of July 31, 2023). The simulated factor paths are then converted into forecasts of $r_t^*$. Figure 14 shows the median projection and the 5th and 95th percentile values for the simulated natural real rate over a ten-year forecast horizon.[18]

The median $r_t^*$ projection shows a very gradual reversal of the declines over the past two decades that brings the natural rate back into positive territory by 2032. The upper 95th percentile rises more rapidly and assumes positive values by 2024, while the lower 5th percentile represents outcomes with the natural real rate remaining persistently in negative territory over the entire forecast horizon. Although stationary, these results show that a highly persistent model like our preferred AFNS-L model can deviate from the estimated mean for several decades. Thus, nonstationary dynamics such as unit roots or trending shifting end points are not necessary to satisfactorily model the secular persistent decline

[18]Note that the lines do not represent short rate paths from a single simulation run over the forecast horizon; instead, they delineate the distribution of all simulation outcomes at a given point in time.

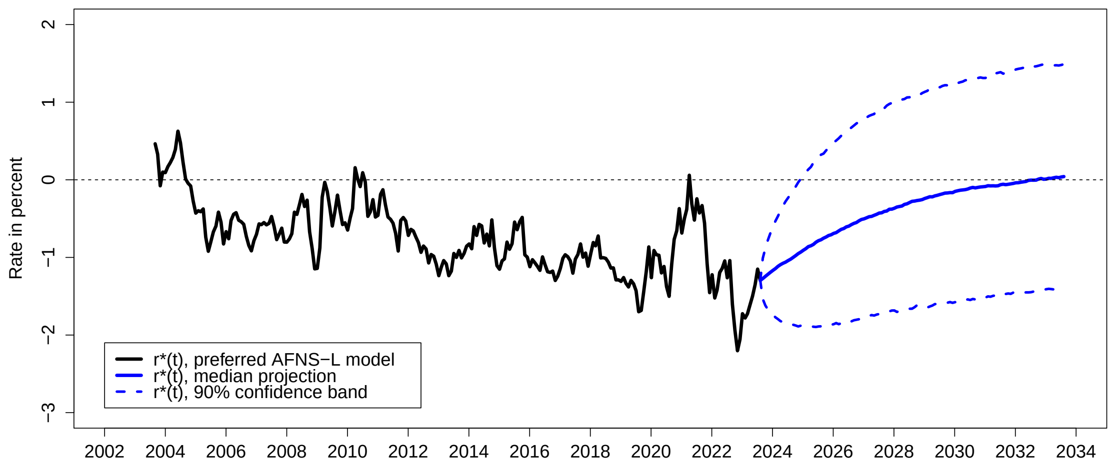


Figure 14: **Ten-Year Projections of r* from AFNS-L Model**

of interest rates observed in the Chilean inflation-indexed bond market over the past two decades. Of course, like most estimates of persistent dynamics, the model may still suffer from some finite-sample bias in the estimated parameters of its mean-reversion matrix $K^{\mathbb{P}}$, which would imply that it does not exhibit a sufficient amount of persistence—as described in Bauer et al. (2012). In turn, this would suggest (all else being equal) that the outcomes below the median are more likely than a straight read of the simulated probabilities would indicate, and correspondingly those above the median are less likely than indicated. As a consequence, we view the projections in Figure 14 as an upper bound estimate of the true probability distribution of the future path for the natural real rate. Thus, we consider it even more likely that the natural rate in Chile will remain at or near its current new low for the foreseeable future.

Finally, our finance-based estimate of $r_t^*$ appears relevant to the debate about the source of the decline in the equilibrium real rate. In particular, although our measure of the real rate fluctuated a bit in the immediate aftermath of the financial crisis, our average $r_t^*$ estimate in 2010 is not much different than in 2007 and 2008. This relative stability before and after the financial crisis suggests that flight-to-safety and safety premium explanations of the lower equilibrium real rate are unlikely to be key drivers of the downtrend in Chilean interest rates during this period. Instead, our estimate appears more broadly consistent with many of the explanations that attribute the decline in the natural rate to real-side fundamentals such as changing demographics (e.g., Carvalho et al. 2016, Favero et al. 2016, and Gagnon et al. 2016).[19] Moreover, once inflation is brought back under control, our results suggest that

[19]World Bank data show that the fertility rate in Chile dropped below 2 births per woman in the early 2000s

real interest rates in Chile—and possibly elsewhere—are likely to return to their pre-pandemic lows, as has also been suggested by Blanchard (2023).

# 6 Conclusion

Given the historic downward trend in bond yields in the decades before the COVID-19 pandemic, many researchers investigated the factors pushing down the steady-state level of the safe short-term real interest rate. However, because most of this empirical work was based on *macroeconomic* models and data, uncertainty about the correct macroeconomic specification—in particular during the COVID-19 pandemic shock—has led some to question the resulting macro-based estimates of the natural rate. We avoid this debate by focusing on a finance-based measure of the equilibrium real rate that is based on empirical dynamic term structure models estimated solely on the prices of inflation-indexed bonds. By adjusting for both inflation-indexed bond liquidity premia and real term premia, we uncover investors' expectations for the underlying frictionless real short rate for the five-year period starting five years ahead. This measure of the natural rate of interest exhibits a gradual decline over the two decades leading up to the pandemic that accounts for about half of the general decline in Chilean government bond yields. Specifically, as of the end of July 2023, the AFNS-L model estimate of $r_t^*$ in Chile is -1.30 percent with a decline greater than 2 percentage points since the beginning of the 2000s. Importantly, projections of this measure of $r_t^*$ show only a very gradual reversal over the coming decade. This suggests that Chilean—and possibly global—long-term interest rates are likely to return to their pre-pandemic lows once inflation is brought back under control, an issue of immense importance to both fiscal policy and long-term asset management.

As for the liquidity premium of the Chilean inflation-indexed bonds, we find it to be large and time varying. Furthermore, regression analysis suggests that it is decreasing in the supply of indexed bonds and positively correlated with the concentration of the amount held by buy-and-hold investors as proxied by pension fund holdings. These results point to large structural frictions in the market for these bonds and underscore the importance of the liquidity adjustment for our analysis.

Given that our measure of the natural rate of interest is based on the forward-looking information priced into the active Chilean inflation-indexed bond market and can be updated at daily frequency, it could serve as an important input for real-time monetary policy analysis and general financial market monitoring. For future research, our methods could also be expanded along an international dimension. With a significant degree of capital mobility, the natural real rate will depend on global saving and investment, so the joint modeling

and has been steadily declining since then reaching 1.54 by 2020.

of inflation-indexed bonds in several countries could be informative (see HLW for an international discussion of the natural rate). Finally, our measure could be incorporated into an expanded joint macroeconomic and finance analysis—particularly with an eye towards further understanding the determinants of any post-pandemic new normal for interest rates.

# References


Andreasen, Martin M. and Jens H. E. Christensen, 2016, "TIPS Liquidity and the Outlook for Inflation," *FRBSF Economic Letter* 2016-35, 1-5.

Andreasen, Martin M., Jens H. E. Christensen, and Simon Riddell, 2021, "The TIPS Liquidity Premium," *Review of Finance*, Vol. 25, No. 6, 1639-1675.

Andreasen, Martin M., Jens H. E. Christensen, and Glenn D. Rudebusch, 2019, "Term Structure Analysis with Big Data: One-Step Estimation Using Bond Prices," *Journal of Econometrics*, Vol. 212, 26-46.

Bauer, Michael D., Glenn D. Rudebusch, and Jing (Cynthia) Wu, 2012, "Correcting Estimation Bias in Dynamic Term Structure Models," *Journal of Business and Economic Statistics*, Vol. 30, No. 3, 454-467.

Beauregard, Remy, Jens H. E. Christensen, Eric Fischer, and Simon Zhu, 2023, "Inflation Expectations and Risk Premia in Emerging Bond Markets: Evidence from Mexico," forthcoming *Journal of International Economics*.

Blanchard, Olivier, 2023, *Fiscal Policy under Low Interest Rates*. MIT Press: Cambridge, Massachusetts.

Campbell, John Y., Robert J. Shiller, and Luis M. Viceira, 2009, "Understanding Inflation-Indexed Bond Markets," *Brookings Papers on Economic Activity*, Spring, 79-120.

Cardozo, Cristhian H. R. and Jens H. E. Christensen, 2023, "The Benefit of Inflation-Indexed Debt: Evidence from an Emerging Bond Market," Working Paper 2023-04, Federal Reserve Bank of San Francisco.

Carvalho, Carlos, Andrea Ferrero, and Fernanda Nechio, 2016, "Demographics and Real Interest Rates: Inspecting the Mechanism," *European Economic Review*, Vol. 88, 208-226.

Christensen, Jens H. E., Francis X. Diebold, and Glenn D. Rudebusch, 2011, "The Affine Arbitrage-Free Class of Nelson-Siegel Term Structure Models," *Journal of Econometrics*, Vol. 164, No. 1, 4-20.

Christensen, Jens H. E., Jose A. Lopez, and Paul L. Mussche, 2022, "Extrapolating Long-Maturity Bond Yields for Financial Risk Measurement," *Management Science*, Vol. 68, No. 11, 8286-8300.

Christensen, Jens H. E., Jose A. Lopez, and Glenn D. Rudebusch, 2014, "Do Central Bank Liquidity Facilities Affect Interbank Lending Rates?," *Journal of Business and Economic Statistics*, Vol. 32, No. 1, 136-151.

Christensen, Jens H. E. and Glenn D. Rudebusch, 2019, "A New Normal for Interest Rates? Evidence from Inflation-Indexed Debt," *Review of Economics and Statistics*, Vol. 101, No. 5, 933-949.

Clarida, Richard, 2014, "Navigating the New Neutral, " *Economic Outlook,* PIMCO, November.

Dai, Qiang and Kenneth J. Singleton, 2000, "Specification Analysis of Affine Term Structure Models," *Journal of Finance*, Vol. 55, No. 5, 1943-1978.

De Pooter, Michiel, Patrice Robitaille, Ian Walker, and Michael Zdinak, 2014, "Are Long-Term Inflation Expectations Well Anchored in Brazil, Chile, and Mexico?," *International Journal of Central Banking*, Vol. 10, No. 2, 337-400.

Driessen, Joost, Theo E. Nijman, and Zorka Simon, 2016, "The Missing Piece of the Puzzle: Liquidity Premiums in Inflation-Indexed Markets," Manuscript, Department of Finance, Tilburg University.

Dudley, William C., Jennifer Roush, and Michelle Steinberg Ezer, 2009, "The Case for TIPS: An Examination of the Costs and Benefits," *Federal Reserve Bank of New York Economic Policy Review*, Vol. 15, No. 1, 1-17.

Duffee, Gregory R., 2002, "Term Premia and Interest Rate Forecasts in Affine Models," *Journal of Finance*, Vol. 57, No. 1, 405-443.

Eggertsson, Gauti B., Neil R. Mehrotra, Sanjay R. Singh, and Lawrence H. Summers, 2016, "A Contagious Malady? Open Economy Discussions of Secular Stagnation," *IMF Economic Review*, Vol. 64, No. 4, 581-634.

Favero, Carlo A., Arie E. Gozluklu, and Haoxi Yang, 2016, "Demographics and the Behavior of Interest Rates," *IMF Economic Review*, Vol. 64, No. 4, 732-776.

Finlay, Richard and Sebastian Wende, 2012, "Estimating Inflation Expectations with a Limited Number of Inflation-Indexed Bonds," *International Journal of Central Banking*, Vol. 8, No. 2, 111-142.

Fleckenstein, Mathias, Francis A. Longstaff, and Hanno Lustig, 2014, "The TIPS-Treasury Bond Puzzle," *Journal of Finance*, Vol. 69, No. 5, 2151-2197.

Fontaine, Jean-Sébastien and René Garcia, 2012, "Bond Liquidity Premia," *Review of Financial Studies*, Vol. 25, No. 4, 1207-1254.

Gagnon, Etienne, Benjamin K. Johannsen, and David Lopez-Salido, 2016, "Understanding the New Normal: The Role of Demographics," Finance and Economics Discussion Series 2016-080. Washington: Board of Governors of the Federal Reserve System, http://dx.doi.org/10.17016/FEDS.2016.080.

Grishchenko, Olesya V. and Jing-Zhi Huang, 2013, "Inflation Risk Premium: Evidence from the TIPS Market," *Journal of Fixed Income*, Vol. 22, No. 4, 5-30.

Gürkaynak, Refet S., Brian Sack, and Jonathan H. Wright, 2010, "The TIPS Yield Curve and Inflation Compensation," *American Economic Journal: Macroeconomics*, Vol. 2, No. 1, 70-92.

Hamilton, James D., Ethan S. Harris, Jan Hatzius, and Kenneth D. West, 2016, "The Equilibrium Real Funds Rate: Past, Present, and Future," *IMF Economic Review*, Vol. 64, No. 4, 660-707.

Holston, Kathryn, Thomas Laubach, and John C. Williams, 2017, "Measuring the Natural Rate of Interest: International Trends and Determinants," *Journal of International Economics*, Vol. 108, 559-575.

Houweling, Patrick, Albert Mentink, and Ton Vorst, 2005, "Comparing Possible Proxies of Corporate Bond Liquidity," *Journal of Banking and Finance*, Vol. 29, 1331-1358.

Hu, Grace X., Jun Pan, and Jiang Wang, 2013, "Noise as Information for Illiquidity," *Journal of Finance*, Vol. 68, No. 6, 2341-2382.

Joslin, Scott, Kenneth J. Singleton, and Haoxiang Zhu, 2011, "A New Perspective on Gaussian Dynamic Term Structure Models," *Review of Financial Studies*, Vol. 24, No. 3, 926-970.

Kiley, Michael T., 2015, "What Can the Data Tell Us About the Equilibrium Real Interest Rate?," Working Paper Finance and Economics Discussion Series 2015-077, Board of Governors of the Federal Reserve System.

Kim, Don H. and Kenneth J. Singleton, 2012, "Term Structure Models and the Zero Bound: An Empirical Investigation of Japanese Yields," *Journal of Econometrics*, Vol. 170, No. 1, 32-49.

Laubach, Thomas and John C. Williams, 2003, "Measuring the Natural Rate of Interest," *Review of Economics and Statistics*, Vol. 85, No. 4, 1063-1070.

Laubach, Thomas and John C. Williams, 2016, "Measuring the Natural Rate of Interest Redux," *Business Economics*, Vol. 51, No. 2, 57-67.

Litterman, Robert and José A. Scheinkman, 1991, "Common Factors Affecting Bond Returns," *Journal of Fixed Income*, Vol. 1, 62-74.

Lo, Stephanie and Kenneth Rogoff, 2015, "Secular Stagnation, Debt Overhang and Other Rationales for Sluggish Growth, Six Years On," Bank for International Settlements, Working Paper No. 482.

Nagel, Stefan, 2016, "The Liquidity Premium of Near-Money Assets," *Quarterly Journal of Economics*, Vol. 131, No. 4, 1927-1971.

Nelson, Charles R. and Andrew F. Siegel, 1987, "Parsimonious Modeling of Yield Curves," *Journal of Business*, Vol. 60, No. 4, 473-489.

Orphanides, Athanasios and John C. Williams, 2002, "Robust Monetary Policy Rules with Unknown Natural Rates," *Brookings Papers on Economic Activity* 2002(2), 63-145.

Pescatori, Andrea and Jarkko Turunen, 2016, "Lower for Longer: Neutral Rate in the U.S.," *IMF Economic Review* Vol. 64, No. 4, 708-731.

Pflueger, Carolin E. and Luis M. Viceira, 2016, "Return Predictability in the Treasury Market: Real Rates, Inflation, and Liquidity," in Handbook of Fixed-Income Securities, edited by P. Veronesi, Wiley, Hoboken, N.J., 191-209 (Chapter 10).

Pritsker, Matt, 2002, "Large Investors and Liquidity: A Review of the Literature," In Committee on the Global Financial System (ed) Risk Measurement and Systematic Risk—Proceedings of the Third Joint Central Bank Research Conference. Bank for International Settlements, Basel, Switzerland, 126-139.

Rachel, Lukasz and Thomas D Smith, 2015, "Secular Drivers of the Global Real Interest Rate," Staff Working Paper 571, Bank of England.

Rudebusch, Glenn D., 2001, "Is the Fed Too Timid? Monetary Policy in an Uncertain World," *Review of Economics and Statistics*, Vol. 83, No. 2, 203-217.

Sack, Brian and Robert Elsasser, 2004, "Treasury Inflation-Indexed Debt: A Review of the U.S. Experience," *Federal Reserve Bank of New York Economic Policy Review*, Vol. 10, No. 1, 47-63.

Shiller, Robert J., 2003, "The Invention of Inflation-Indexed Bonds in Early America," NBER Working Paper No. 10183.

Summers, Lawrence H., 2023, "Back to Secular Stagnation?," Speech at the Annual Meeting of the American Economic Association, January 7, 2023.

Svensson, Lars E. O., 1995, "Estimating Forward Interest Rates with the Extended Nelson-Siegel Method," *Quarterly Review*, No. 3, Sveriges Riksbank, 13-26.

Taylor, John B. and Volker Wieland, 2016, "Finding the Equilibrium Real Interest Rate in a Fog of Policy Deviations," Discussion paper 11264, Centre for Economic Policy Research.

Vayanos, Dimitri and Jean-Luc Vila, 2021, "A Preferred-Habitat Model of the Term Structure of Interest Rates," *Econometrica*, Vol. 89, No. 1, 77-112.